

A Deeper Look at Discounting Mismatch in Actor-Critic Algorithms

Shangdong Zhang^{†1} Romain Laroche² Harm van Seijen² Shimon Whiteson¹ Remi Tachet des Combes²

Abstract

We investigate the discounting mismatch in actor-critic algorithm implementations from a representation learning perspective. Theoretically, actor-critic algorithms usually have discounting for both the actor and critic, *i.e.*, there is a γ^t term in the actor update for the transition observed at time t in a trajectory and the critic is a discounted value function. Practitioners, however, usually ignore the discounting (γ^t) for the actor while using a discounted critic. We investigate this mismatch in two scenarios. In the first scenario, we consider optimizing an undiscounted objective ($\gamma = 1$) where γ^t disappears naturally ($1^t = 1$). We then propose to interpret the discounting in the critic in terms of a *bias-variance-representation* trade-off and provide supporting empirical results. In the second scenario, we consider optimizing a discounted objective ($\gamma < 1$) and propose to interpret the omission of the discounting in the actor update from an *auxiliary task* perspective and provide supporting empirical results.

1. Introduction

Actor-critic algorithms have enjoyed great success both theoretically (Williams, 1992; Sutton et al., 2000; Konda, 2002; Schulman et al., 2015a) and empirically (Mnih et al., 2016; Silver et al., 2016; Schulman et al., 2017; OpenAI, 2018). There is, however, a longstanding gap between the theory behind actor-critic algorithms and how practitioners implement them. Let γ , γ_A , and γ_C be the discount factors for defining the objective, updating the actor, and updating the critic respectively. Theoretically, no matter whether $\gamma = 1$ or $\gamma < 1$, we should always use $\gamma_A = \gamma_C = \gamma$ (Sutton et al., 2000; Schulman et al., 2015a) or at least keep $\gamma_A = \gamma_C$ if Blackwell optimality (Veinott, 1969; Weitzman,

2001)³ is considered. Practitioners, however, usually use $\gamma_A = 1$ and $\gamma_C < 1$ in their implementations (Dhariwal et al., 2017; Caspi et al., 2017; Zhang, 2018; Kostrikov, 2018; Achiam, 2018; Liang et al., 2018; Stooke & Abbeel, 2019). Although this mismatch and its theoretical disadvantage have been recognized by Thomas (2014); Nota & Thomas (2020), whether and why it yields benefits in practice has not been systematically studied. In this paper, we empirically investigate this mismatch from a representation learning perspective. We consider two scenarios separately.

Scenario 1: *The true objective is undiscounted ($\gamma = 1$).* The theory prescribes to use $\gamma_A = \gamma_C = \gamma = 1$. Practitioners, however, usually use $\gamma_A = \gamma = 1$ but $\gamma_C < 1$, introducing *bias*. We explain this mismatch with the following hypothesis:

Hypothesis 1. $\gamma_C < 1$ optimizes a *bias-variance-representation trade-off*.

It is easy to see that $\gamma_C < 1$ reduces the variance in bootstrapping targets. We also provide empirical evidence showing that when $\gamma_C < 1$, it may become easier to find a good representation than when $\gamma_C = 1$, for reasons beyond the reduced variance. Consequently, although using $\gamma_C < 1$ introduces bias, it can facilitate representation learning. For our empirical study, we make use of recently introduced techniques, such fixed horizon temporal difference learning (De Asis et al., 2019) and distributional reinforcement learning (Bellemare et al., 2017) to disentangle the various effects of the discount factor on the learning process.

Scenario 2: *The true objective function is discounted ($\gamma < 1$).* Theoretically, there is a γ^t term for the actor update on a transition observed at time t in a trajectory (Sutton et al., 2000; Schulman et al., 2015a). Practitioners, however, usually ignore this term while using a discounted critic, *i.e.*, $\gamma_A = 1$ and $\gamma_C = \gamma < 1$ are used. We explain this mismatch with the following hypothesis:

Hypothesis 2. *Using $\gamma_C = \gamma < 1$ and $\gamma_A = 1$ is effectively similar to using $\gamma_C = \gamma_A = \gamma < 1$ plus an auxiliary loss that sometimes facilitates representation learning.*

Our empirical study involves implementing the auxiliary

[†]Part of this work was done during an internship at Microsoft Research Montreal. ¹University of Oxford ²Microsoft Research, Montreal. Correspondence to: Shangdong Zhang <shangdong.zhang@cs.ox.ac.uk>, Remi Tachet des Combes <remi.tachet@microsoft.com>.

³Blackwell optimality states that, in finite MDPs, there exists a $\gamma_0 < 1$ such that for all $\gamma \geq \gamma_0$, the optimal policies for the γ -discounted objective are the same.

task explicitly by using an additional policy for optimizing the difference term between the loss of $\gamma_A = 1$ and the loss of $\gamma_A < 1$. We also design new benchmarking environments where the sign of the reward function is flipped after a certain time step such that later transitions differ from earlier ones. In that setting, $\gamma_A = 1$ becomes harmful.

2. Background

Markov Decision Processes: We consider an infinite horizon MDP with a finite state space \mathcal{S} , a finite action space \mathcal{A} , a bounded reward function $r : \mathcal{S} \rightarrow \mathbb{R}$, a transition kernel $p : \mathcal{S} \times \mathcal{S} \times \mathcal{A} \rightarrow [0, 1]$, an initial state distribution μ_0 , and a discount factor $\gamma \in [0, 1]$.⁴ The initial state S_0 is sampled from μ_0 . At time step t , an agent in state S_t takes action $A_t \sim \pi(\cdot|S_t)$, where $\pi : \mathcal{A} \times \mathcal{S} \rightarrow [0, 1]$ is the policy it follows. The agent then gets a reward $R_{t+1} \doteq r(S_t)$ and proceeds to the next state $S_{t+1} \sim p(\cdot|S_t, A_t)$. The return of the policy π at time step t is defined as $G_t \doteq \sum_{i=1}^{\infty} \gamma^{i-1} R_{t+i}$, which allows us to define the state value function $v_{\pi}^{\gamma}(S) \doteq \mathbb{E}[G_t|S_t = s]$ and the state-action value function $q_{\pi}^{\gamma}(s, a) \doteq \mathbb{E}[G_t|S_t = s, A_t = a]$. We consider episodic tasks where we assume there is an absorbing state $s^{\infty} \in \mathcal{S}$ such that $r(s^{\infty}) = 0$ and $p(s^{\infty}|s^{\infty}, a) = 1$ holds for any $a \in \mathcal{A}$. When $\gamma < 1$, v_{π}^{γ} and q_{π}^{γ} are always well defined. When $\gamma = 1$, to ensure v_{π}^{γ} and q_{π}^{γ} are well defined, we further assume finite expected episode length. Let T_s^{π} be a random variable denoting the first time step that an agent hits s^{∞} when following π given $S_0 = s$. We assume $T_{\max} \doteq \sup_{\pi \in \Pi} \max_s \mathbb{E}[T_s^{\pi}] < \infty$, where π is parameterized by θ and Π is the corresponding function class. Similar assumptions are also used in stochastic shortest path problems (e.g., Section 2.2 of Bertsekas & Tsitsiklis (1996)). In our experiments, all the environments have a hard time limit of 1000, i.e., $T_{\max} = 1000$. This is standard practice; classic RL environments also have an upper limit on their episode lengths (e.g. 27k in Bellemare et al. (2013, ALE)). Following Pardo et al. (2018), we add the (normalized) time step t in the state to keep the environment Markovian. We measure the performance of a policy π with $J_{\gamma}(\pi) \doteq \mathbb{E}_{S_0 \sim \mu_0}[v_{\pi}^{\gamma}(S_0)]$.

Vanilla Policy Gradient: Sutton et al. (2000) compute $\nabla_{\theta} J_{\gamma}(\pi)$ as

$$\nabla_{\theta} J_{\gamma}(\pi) \doteq \sum_s d_{\pi}^{\gamma}(s) \sum_a q_{\pi}^{\gamma}(s, a) \nabla_{\theta} \pi(a|s), \quad (1)$$

where $d_{\pi}^{\gamma}(s) \doteq \sum_{t=0}^{\infty} \gamma^t \Pr(S_t = s | \mu_0, p, \pi)$ for $\gamma < 1$ and $d_{\pi}^{\gamma}(s) \doteq \mathbb{E}[\sum_{t=0}^{T_s^{\pi}} \Pr(S_t = s | S_0, p, \pi)]$ for $\gamma = 1$.⁵ Note d_{π}^{γ} remains well-defined for $\gamma = 1$ when $T_{\max} < \infty$. In

⁴Following Schulman et al. (2015a), we consider $r : \mathcal{S} \rightarrow \mathbb{R}$ instead of $r : \mathcal{S} \times \mathcal{A} \rightarrow \mathbb{R}$ for simplicity.

⁵Sutton et al. (2000) do not explicitly define d_{π}^{γ} when $\gamma = 1$, which, however, can be easily deduced from Chapter 13.2 in Sutton & Barto (2018).

order to optimize the policy performance $J_{\gamma}(\pi)$, one can follow (1) and, at time step t , update θ_t as

$$\theta_{t+1} \leftarrow \theta_t + \alpha \gamma_A^t q_{\pi}^{\gamma_c}(S_t, A_t) \nabla_{\theta} \log \pi(A_t | S_t), \quad (2)$$

where α is a learning rate. If we replace $q_{\pi}^{\gamma_c}$ with a learned value function, the update rule (2) becomes an actor-critic algorithm, where the actor refers to π and the critic refers to the learned approximation of $q_{\pi}^{\gamma_c}$. In practice, an estimate for $v_{\pi}^{\gamma_c}$ instead of $q_{\pi}^{\gamma_c}$ is usually learned. Theoretically, we should have $\gamma_A = \gamma_c = \gamma$. Practitioners, however, usually ignore the γ_A^t term in (2), and use $\gamma_c < \gamma_A = 1$. What this update truly optimizes remains an open problem (Nota & Thomas, 2020).

TRPO and PPO: To improve the stability of actor-critic algorithms, Schulman et al. (2015a) propose Trust Region Policy Optimization (TRPO), based on the performance improvement lemma:

Lemma 1. (Theorem 1 in Schulman et al. (2015a)) For $\gamma < 1$ and any two policies π and π' ,

$$J_{\gamma}(\pi') \geq J_{\gamma}(\pi) + \sum_s d_{\pi}^{\gamma}(s) \sum_a \pi'(a|s) \text{Adv}_{\pi}^{\gamma}(s, a) - \frac{4 \max_{s,a} |\text{Adv}_{\pi}^{\gamma}(s, a)| \gamma \epsilon(\pi, \pi')}{(1-\gamma)^2},$$

where $\text{Adv}_{\pi}^{\gamma}(s, a) \doteq \mathbb{E}_{s' \sim p(\cdot|s,a)}[r(s) + \gamma v_{\pi}^{\gamma}(s') - v_{\pi}^{\gamma}(s)]$ is the advantage, $\epsilon(\pi, \pi') \doteq \max_s D_{KL}(\pi(\cdot|s) || \pi'(\cdot|s))$, and D_{KL} refers to the KL divergence.

To facilitate our empirical study, we first make a theoretical contribution by extending Lemma 1 to the undiscounted setting. We have the following lemma:

Lemma 2. Assuming $T_{\max} < \infty$, for $\gamma = 1$ and any two policies π and π' ,

$$J_{\gamma}(\pi') \geq J_{\gamma}(\pi) + \sum_s d_{\pi}^{\gamma}(s) \sum_a \pi'(a|s) \text{Adv}_{\pi}^{\gamma}(s, a) - 4 \max_{s,a} |\text{Adv}_{\pi}^{\gamma}(s, a)| T_{\max}^2 \epsilon(\pi, \pi').$$

The proof of Lemma 2 is provided in the appendix. A practical implementation of Lemmas 1 and 2 is to compute a new policy θ via gradient ascent on the clipped objective:

$$L(\theta) \doteq \sum_{t=0}^{\infty} \gamma_A^t L_t(\theta, \theta_{\text{old}}), \text{ where} \quad (3)$$

$$L_t(\theta, \theta_{\text{old}}) \doteq \min \left\{ \frac{\pi_{\theta}(A_t|S_t)}{\pi_{\theta_{\text{old}}}(A_t|S_t)} \text{Adv}_{\pi_{\theta_{\text{old}}}}^{\gamma_c}(S_t, A_t), \right.$$

$$\left. \text{clip}\left(\frac{\pi_{\theta}(A_t|S_t)}{\pi_{\theta_{\text{old}}}(A_t|S_t)}\right) \text{Adv}_{\pi_{\theta_{\text{old}}}}^{\gamma_c}(S_t, A_t) \right\}.$$

Here S_t and A_t are sampled from $\pi_{\theta_{\text{old}}}$, and $\text{clip}(x) \doteq \max(\min(x, 1 + \epsilon), 1 - \epsilon)$ with ϵ a hyperparameter. Theoretically, we should have $\gamma_A = \gamma_c$, but practical algorithms like Proximal Policy Optimization (Schulman et al., 2017, PPO) usually use $\gamma_c < \gamma_A = 1$.

Policy Evaluation: We now introduce several policy evaluation techniques we use in our empirical study. Let \hat{v}

be our estimate of v_π^γ . At time step t , Temporal Difference learning (TD, Sutton (1988)) updates \hat{v} as $\hat{v}(S_t) \leftarrow \hat{v}(S_t) + \alpha(R_{t+1} + \gamma\hat{v}(S_{t+1}) - \hat{v}(S_t))$. Instead of the infinite horizon discounted return G_t , De Asis et al. (2019) propose to consider the H -step return $G_t^H \doteq \sum_{i=1}^H R_{t+i}$. Correspondingly, the H -step value function is defined as $v_\pi^H(s) \doteq \mathbb{E}[G_t^H | S_t = s]$. We let \hat{v}^H be our estimate of v_π^H . At time step t , De Asis et al. (2019) use the following update rule to learn \hat{v}^H . For $i = 1, \dots, H$:

$$\hat{v}^i(S_t) \leftarrow \hat{v}^i(S_t) + \alpha(R_{t+1} + \hat{v}^{i-1}(S_{t+1}) - \hat{v}^i(S_t)), \quad (4)$$

where $\hat{v}^0(s) \doteq 0$. In other words, to learn \hat{v}^H , we need to learn $\{\hat{v}^i\}_{i=1, \dots, H}$ simultaneously. De Asis et al. (2019) call (4) *Fixed Horizon Temporal Difference learning (FHTD)*.

As G_t is a random variable, Bellemare et al. (2017) propose to learn its full distribution instead of its expectation only, yielding the Distributional Reinforcement Learning (RL) paradigm. They use a categorical distribution with 51 atoms uniformly distributed in $[-V_{\max}, V_{\max}]$ to approximate the distribution of G_t , where V_{\max} is a hyperparameter. In this paper, we refer to the corresponding policy evaluation algorithm as *C51*.

Methodology: We consider MuJoCo robot simulation tasks from OpenAI gym (Brockman et al., 2016) as our benchmark. Given its popularity in understanding deep RL algorithms (Henderson et al., 2017; Ilyas et al., 2018; Engstrom et al., 2019; Andrychowicz et al., 2020) and designing new deep RL algorithms (Fujimoto et al., 2018; Haarnoja et al., 2018), we believe our empirical results are relevant to most practitioners.

We choose PPO, a simple yet effective and widely used algorithm, as the representative actor-critic algorithm for our empirical study. PPO is usually equipped with generalized advantage estimation (Schulman et al., 2015b, GAE), which has a tunable hyperparameter $\hat{\gamma}$. The roles of γ and $\hat{\gamma}$ are similar. To reduce its confounding effect, we do not use GAE in our experiments, *i.e.*, the advantage estimation for our actor is simply the TD error $R_{t+1} + \gamma\hat{v}(S_{t+1}) - \hat{v}(S_t)$. The PPO pseudocode we follow is provided in Alg. 1 in the appendix and we refer to it as the default PPO implementation.

We use the standard architecture and optimizer across all tasks. In particular, the actor and the critic do not share layers. We conduct a thorough learning rate search in `Ant` for each algorithmic configuration (*i.e.*, a curve in a figure) and then use the same learning rate for all other tasks. Section B.1 in the appendix empirically shows that the best learning rate in `Ant` is reasonably good for other tasks. When using FHTD and C51, we also include H and V_{\max} in the grid search. All details are provided in the appendix. We report the average episode return of the ten most recent

episodes against the number of interactions with the environment. Curves are averages over ten independent runs with shaded regions indicating standard errors.

3. Optimizing the Undiscounted Objective (Scenario 1)

In this scenario, the goal is to optimize the *undiscounted* objective $J_{\gamma=1}(\pi)$. This scenario is related to most practitioners as they usually use the undiscounted return as the performance metric (Mnih et al., 2016; Schulman et al., 2017; Haarnoja et al., 2018). One theoretically grounded option is to use $\gamma_A = \gamma_C = \gamma = 1$. By using $\gamma_A = 1$ and $\gamma_C < 1$, practitioners introduce *bias*. We first empirically confirm that introducing bias in this way indeed has empirical advantages. A simple first hypothesis is that $\gamma_C < 1$ leads to lower variance in Monte Carlo return bootstrapping targets than $\gamma_C = 1$; it thus optimizes a bias-variance trade-off. However, we further show that there are empirical advantages from $\gamma_C < 1$ that cannot be uniquely explained by this bias-variance trade-off, indicating that there are additional factors beyond variance. We then show empirical evidence identifying representation learning as an additional factor, leading to the *bias-variance-representation* trade-off from Hypothesis 1. All the experiments in this section use $\gamma_A = 1$.

Bias-variance trade-off: To investigate the advantages of using $\gamma_C < 1$, we first test default PPO with $\gamma_C \in \{0.95, 0.97, 0.99, 0.995, 1\}$. We find that the best discount factor is always with $\gamma_C < 1$ and that $\gamma_C = 1$ usually leads to a performance drop (Figure 1). In default PPO, although the advantage is computed as the one-step TD error, the update target for updating the critic $\hat{v}(S_t)$ is almost always a Monte Carlo return. As there is no γ_A^t term in the actor update, we should theoretically use $\gamma_C = \gamma_A = 1$ when computing the Monte Carlo return, which usually leads to high variance. Consequently, a simple hypothesis for the empirical advantages of using $\gamma_C < 1$ is a bias-variance trade-off. We find, however, that there is more at play.

Beyond bias-variance trade-off: To reduce the effect of γ_C in controlling the variance, we benchmark PPO-TD (Algorithm 2 in the appendix). PPO-TD is the same as default PPO except that the critic is updated with one-step TD, *i.e.*, the update target for $\hat{v}(S_t)$ is now $R_{t+1} + \gamma_C\hat{v}(S_{t+1})$. Although Figure 2 shows that PPO-TD ($\gamma_C = 1$) outperforms PPO ($\gamma_C = 1$) by a large margin, indicating bias-variance may be at play, Figure 3 suggests that for PPO-TD as well, $\gamma_C < 1$ is still preferable to $\gamma_C = 1$. To further study this phenomenon, we benchmark PPO-TD-Ex (Algorithm 3 in the appendix), in which we provide N extra transitions to the critic by sampling multiple actions at any single state and using an averaged bootstrapping target. The update target for $\hat{v}(S_t)$ in PPO-TD-Ex is $\frac{1}{N+1} \sum_{i=0}^N R_{t+1}^i + \gamma_C \hat{v}(S_{t+1}^i)$.

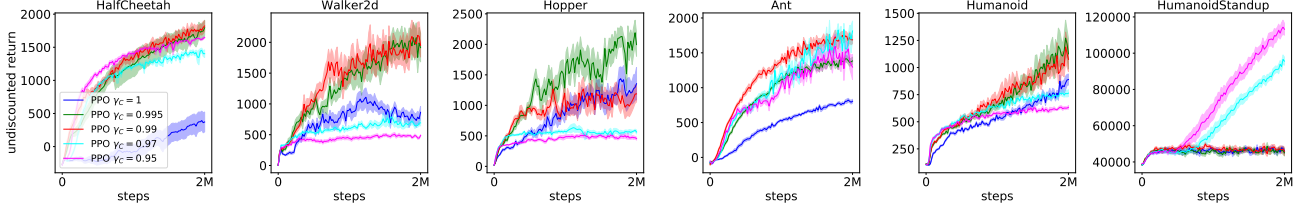


Figure 1: The default PPO implementation with different discount factors.

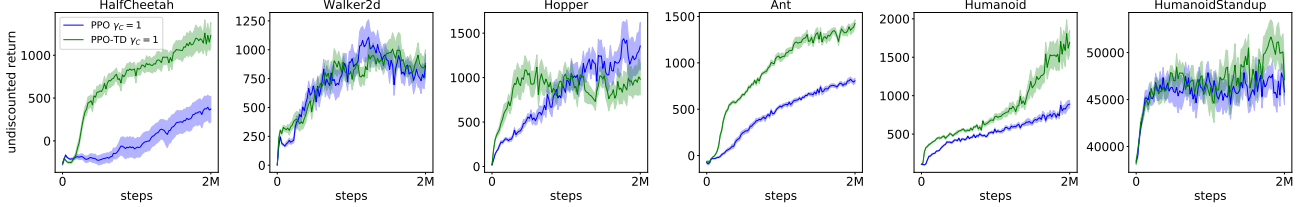
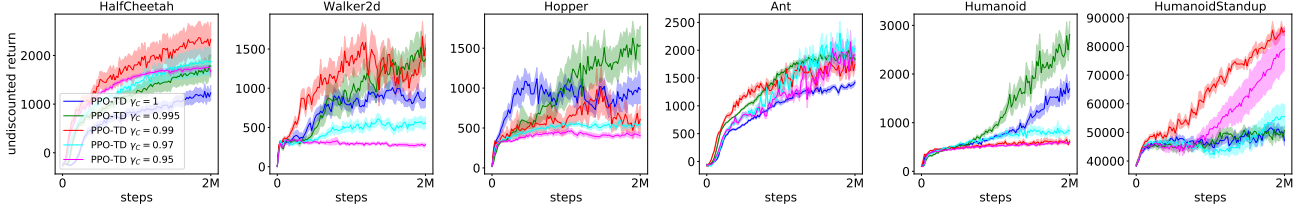
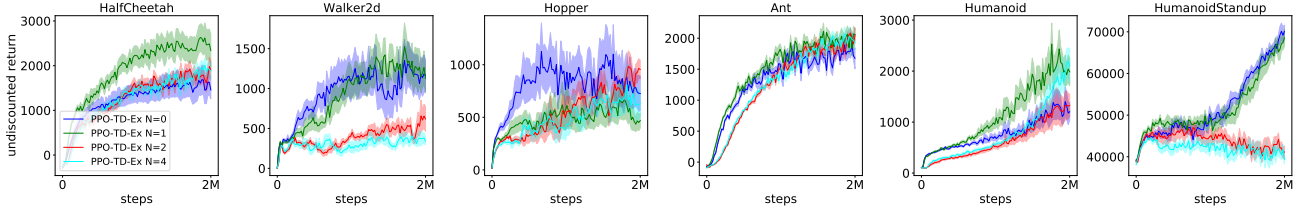
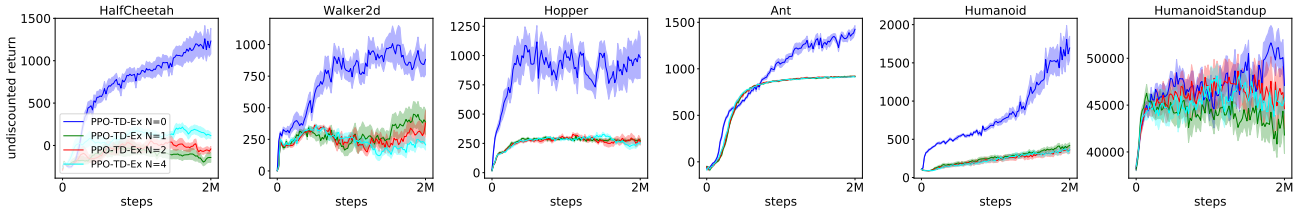

Figure 2: Comparison between PPO and PPO-TD when $\gamma_c = 1$.


Figure 3: PPO-TD with different discount factors.


Figure 4: PPO-TD-Ex ($\gamma_c = 0.99$).

Figure 5: PPO-TD-Ex ($\gamma_c = 1$).

Here R_{t+1}^0 and S_{t+1}^0 refer to the original reward and successor state. To get R_{t+1}^i and S_{t+1}^i for $i \in \{1, \dots, N\}$, we first sample an action A_t^i from the sampling policy, then reset the environment to S_t , and finally execute A_t^i to get R_{t+1}^i and S_{t+1}^i . The advantage for the actor update in PPO-TD-Ex is estimated with $R_{t+1}^0 + \hat{v}(S_{t+1}^0) - \hat{v}(S_t)$ regardless of γ_c

to further control the influence of variance. Importantly, we do not count those N extra transitions in the x -axis when plotting. If we use the true value function instead of \hat{v} , $N \geq 1$ should always outperform $N = 0$ as the additional transitions help reduce variance (assuming γ_c is fixed). However, in practice we have only \hat{v} , which is not

trained on the extra successor states $\{S_{t+1}^i\}_{i=1,\dots,N}$. So the quality of the prediction $\hat{v}(S_{t+1}^i)$ depends mainly on the generalization of \hat{v} . Consequently, increasing N risks potential erroneous prediction $\hat{v}(S_{t+1}^i)$. We, therefore, conclude that an intermediate N could be the sweet spot. As shown by Figure 4, PPO-TD-Ex ($\gamma_c = 0.99$) roughly follows this intuition. However, surprisingly, providing any extra transition this way to PPO-TD-Ex ($\gamma_c = 1$) in general leads to a significant performance drop (Figure 5). This drop suggests that the quality of the critic \hat{v} , at least in terms of making prediction on untrained states $\{S_{t+1}^i\}_{i=1,\dots,N}$, is lower when $\gamma_c = 1$ is used than $\gamma_c < 1$. In other words, the generalization of \hat{v} becomes poorer when γ_c is increased from 0.99 to 1. The curves for PPO-TD-Ex ($\gamma_c = 0.995$) are a mixture of $\gamma_c = 0.99$ and $\gamma_c = 1$ and are provided in Figure 16 in the appendix. The retarded generalization could imply that representation learning becomes harder when γ_c is increased. By representation learning, we refer to learning the bottom layers (backbone) of a neural network. The last layer of the neural network is then interpreted as a linear function approximator whose features are the output of the backbone. This interpretation of representation learning is widely used in the RL community, see, e.g., Jaderberg et al. (2016); Chung et al. (2018); Veeriah et al. (2019).

In PPO-TD, the bootstrapping target for training $\hat{v}(S_t)$ is $R_{t+1} + \gamma_c \hat{v}(S_{t+1})$, where γ_c has two roles. First, it controls how the randomness of S_{t+1} affects the bootstrapping target, which we refer to as *variance control*. Second, it affects the value function $v_\pi^{\gamma_c}$ that we want to approximate via changing the horizon of the policy evaluation problem, which could possibly affect the difficulty of learning a good estimate \hat{v} for $v_\pi^{\gamma_c}$ directly, not through the variance, which we refer to as *learnability control* (see, e.g., (Lehnert et al., 2018; Laroché & van Seijen, 2018; Romoff et al., 2019)). Both roles can be responsible for the increased difficulty in representation learning when γ_c is increased. In the rest of this section, we provide empirical evidence showing that the changed difficulty in representation learning, resulting directly from the changed horizon of the policy evaluation problem, is at play when using the $\gamma_c < 1$, which, together with the previously established bias-variance trade-off, suggests that a *bias-variance-representation trade-off* is at play when practitioners use $\gamma_c < 1$.

To separate the effect on representation learning of learnability control from that of variance control, we use FHTD to train the critic in PPO, which we refer to as PPO-FHTD (Algorithm 4 in the appendix). PPO-FHTD always use $\gamma_c = 1$ regardless of H . And manipulating H changes the horizon of the policy evaluation problem, which corresponds to the role of learnability control.

We test two parameterizations for PPO-FHTD to investigate representation learning. In the first parameterization,

to learn v_π^H , we parameterize $\{v_\pi^i\}_{i=1,\dots,H}$ as H different heads over the same representation layer (backbone). In the second parameterization, we always learn $\{v_\pi^i\}_{i=1,\dots,1024}$ as 1024 different heads over the same representation layer, whatever H we are interested in. To approximate v_π^H , we then simply use the output of the H -th head. A diagram (Figure 13) in the appendix further illustrates the difference between the two parameterizations.

Figure 6 shows that by tuning H for FHTD, PPO-FHTD with the first parameterization matches or exceeds the performance of PPO-TD ($\gamma_c < 1$) in most tasks, and that the best H is always smaller than 1024. Theoretically, as long as we use an $H \geq T_{\max} = 1000$, we always have $v_\pi^H(s) \equiv v_\pi^{\gamma=1}(s)$. Figure 6 shows that the performance of PPO-FHTD ($H = 1024$) is very close to PPO-TD ($\gamma_c = 1$), indicating that learning $\{v_\pi^i\}_{i=1,\dots,1023}$ is not an additional overhead for the network in terms of learning $v_\pi^{H=1024}$, i.e., increasing H does not pose additional challenges in terms of network capacity. However, Figure 7 suggests that for the second parameterization, $H = 1024$ is almost always among the best choices of H . Comparing Figures 6 and 7, we conclude that in the tested domains, learning v_π^H with different H requires different representations. This suggests that we can interpret the results in Figure 6 as a *bias-representation trade-off*. Using a larger H is less biased but representation learning may become harder due to the longer policy evaluation horizon. Consequently, an intermediate H achieves the best performance in Figure 6. As reducing H cannot bring in advantages in representation learning under the second parameterization, the less biased H , i.e., the larger H , usually performs better in Figure 7. Overall, γ_c optimizes a *bias-representation trade-off* by changing the policy evaluation horizon H .

We further conjecture that representation learning may be harder for a longer horizon because good representations can become more sparse. We provide a simulated example to support this. Consider policy evaluation on the simple Markov Reward Process (MRP) from Figure 9. We assume the reward for each transition is fixed, which is randomly generated in $[0, 1]$. Let $x_s \in \mathbb{R}^K$ be the feature vector for a state s ; we set its i -th component as $x_s[i] \doteq \tanh(\xi)$, where ξ is a random variable uniformly distributed in $[-2, 2]$. We choose this feature setup as we use \tanh as the activation function in our PPO. We use $X \in \mathbb{R}^{N \times K}$ to denote the feature matrix. To create state aliasing (McCallum, 1997), which is common under function approximation, we first randomly split the N states into \mathcal{S}_1 and \mathcal{S}_2 such that $|\mathcal{S}_1| = \alpha N$ and $|\mathcal{S}_2| = (1 - \alpha)N$, where α is the proportion of states to be aliased. Then for every $s \in \mathcal{S}_1$, we randomly select an $\hat{s} \in \mathcal{S}_2$ and set $x_s \leftarrow x_{\hat{s}}$. Finally, we

⁶The trend that NRE decreases as α increases is merely an artifact from how we generate v_γ .

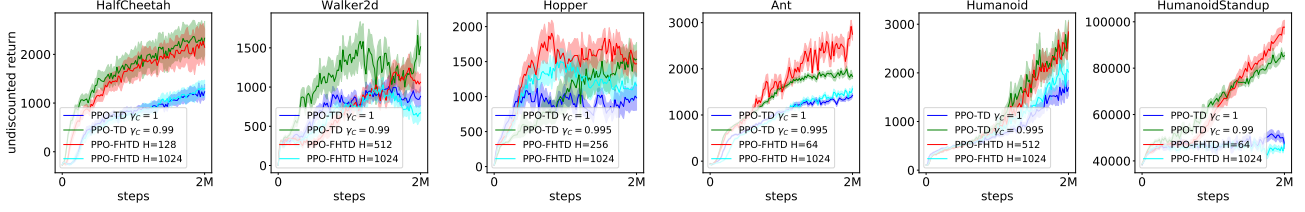


Figure 6: PPO-FHTD with the first parameterization. The best H and γ_c are used for each game.

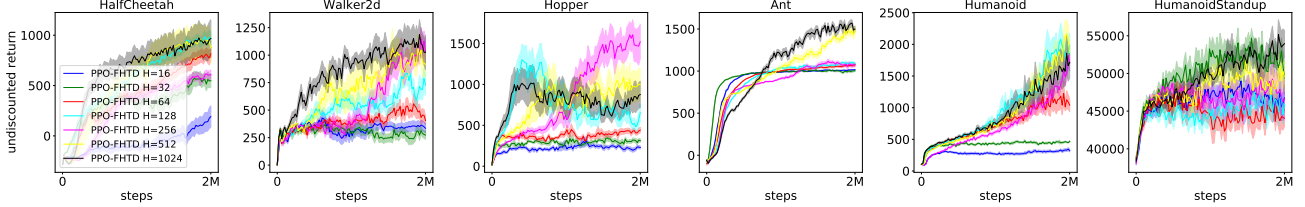


Figure 7: PPO-FHTD with the second parameterization.

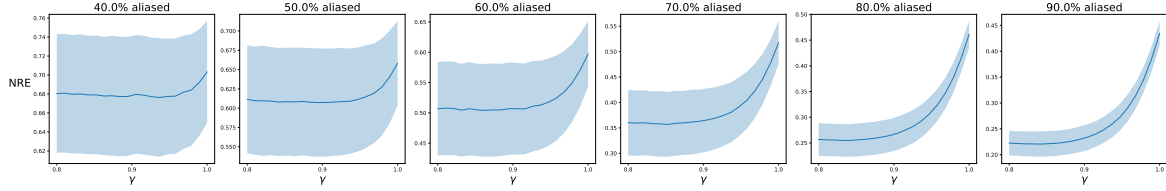


Figure 8: Normalized representation error as a function of the discount factor. Shaded regions indicate one standard derivation.⁶

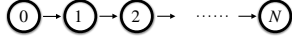


Figure 9: A simple MRP.

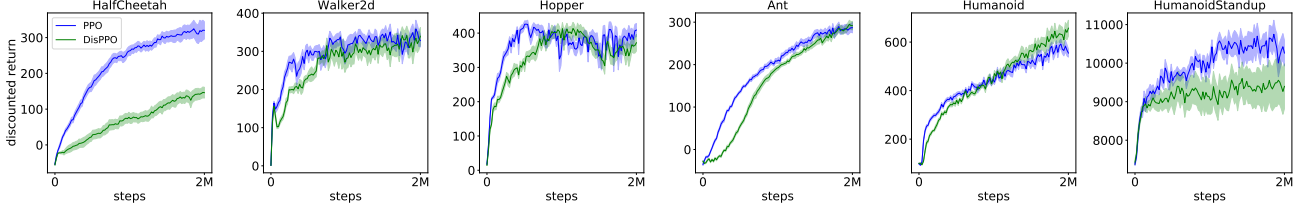
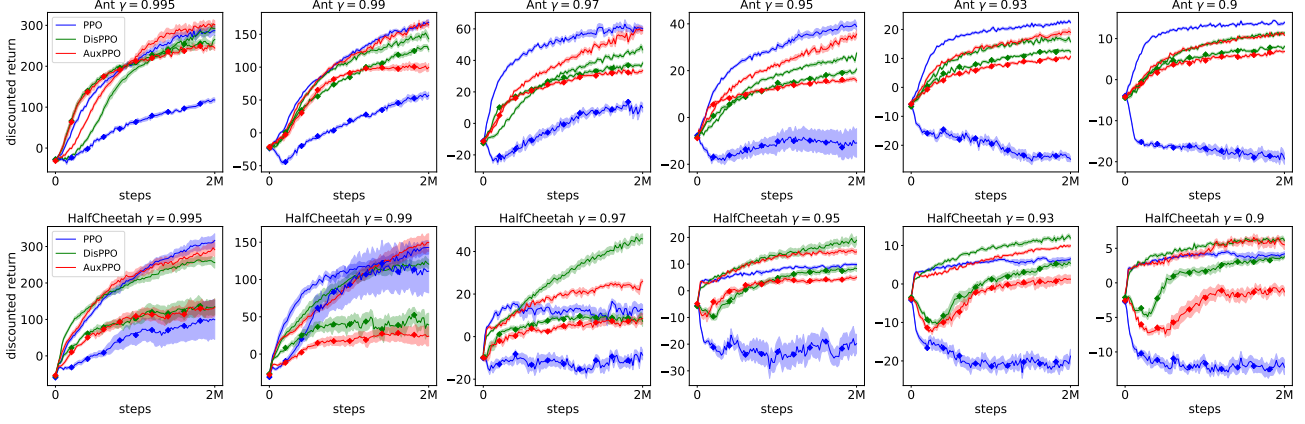
add Gaussian noise $\mathcal{N}(0, 0.1^2)$ to each element of X . We use $N = 100$ and $K = 30$ in our simulation and report the normalized representation error (NRE) as a function of γ . For a feature matrix X , the NRE is computed analytically as $\text{NRE}(\gamma) \doteq \frac{\min_w \|Xw - v_\gamma\|_2}{\|v_\gamma\|_2}$, where v_γ is the analytically computed true value function of the MRP. We report the results in Figure 8, where each data point is averaged over 10^4 randomly generated feature matrices (X) and reward functions. In this MRP, the average representation error becomes larger as γ increases, which suggests that, in this MRP, good representations become more sparse under a larger γ and state than that under a smaller γ . Importantly, in this MRP experiment, we compute all the quantities analytically so no variance is involved within a single trial. Consequently, representation error is a property of v_γ itself. We report the unnormalized representation error in Figure 17 in the appendix, where the trend is much clearer.

⁶See Section B.1 for more details about task selection.

Overall, though we do not claim that there is a monotonic relationship between the discount factor and the difficulty of representation learning, our empirical study does suggest that representation learning is a key factor at play in the misuse of the discounting in actor-critic algorithms, beyond the widely recognized bias-variance trade-off. In the appendix, we provide additional experiments involving distributional RL to further support the bias-variance-representation trade-off hypothesis, under the assumption that the benefits of distributional RL comes mainly from the improved representation learning (Bellemare et al., 2017; Munos, 2018; Petroski Such et al., 2019).

4. Optimizing the Discounted Objective (Scenario 2)

When our goal is to optimize the *discounted* objective $J_{\gamma < 1}(\pi)$, theoretically we should have the γ_A^t term in the actor update and use $\gamma_c < 1$. Practitioners, however, usually ignore this γ_A^t (i.e., set $\gamma_A = 1$), introducing *bias*. Figure 10 shows that even if we use the *discounted* return as the performance metric, the biased implementation of PPO still outperforms the theoretically grounded implementation DisPPO in the domains we tested. Here PPO refers to the


 Figure 10: Comparison between PPO and DisPPO with $\gamma = 0.995$

 Figure 11: Curves without any marker are obtained in the original Ant / HalfCheetah. Diamond-marked curves are obtained in Ant / HalfCheetah with r' .⁷

default PPO implementation where $\gamma_A = 1, \gamma_C = \gamma < 1$, and DisPPO (Alg. 6 in the appendix) adds the missing γ_A^t term in PPO by using $\gamma_A = \gamma_C = \gamma < 1$. We propose to interpret the empirical advantages of PPO over DisPPO with Hypothesis 2. For all experiments in this section, we use $\gamma_C = \gamma < 1$.

An auxiliary task perspective: The biased policy update implementation of (2) ignoring γ_A^t can be decomposed into two parts as $\Delta_t = \gamma^t \Delta_t + (1 - \gamma^t) \Delta_t$, where $\Delta_t \doteq q_{\pi}^{\gamma_C}(S_t, A_t) \nabla_{\theta} \log \pi(A_t | S_t)$. We propose to interpret the *difference term* between the biased implementation (Δ_t) and the theoretically grounded implementation ($\gamma^t \Delta_t$), i.e., the $(1 - \gamma^t) q_{\pi}^{\gamma_C}(S_t, A_t) \nabla_{\theta} \log \pi(A_t | S_t)$ term, as the gradient of an auxiliary objective with a dynamic weighting $1 - \gamma^t$. Let $J_{s,\mu}(\pi) \doteq \sum_a \pi(a|s) q_{\mu}^{\gamma}(s, a)$; we have $\nabla_{\theta} J_{s,\mu}(\pi)|_{\mu=\pi} = \mathbb{E}_{a \sim \pi(\cdot|s)} [q_{\pi}^{\gamma}(s, a) \nabla_{\theta} \log \pi(a|s)]$. This objective changes every time step (through μ). Inspired by the decomposition, we augment PPO with this auxiliary task, yielding AuxPPO (Algorithm 7 and Figure 13 in the appendix). In AuxPPO, we have two policies π and π' parameterized by θ and θ' respectively. The two policies are two heads over the same neural network backbone, where π is used for interaction with the environment and π' is the policy for the auxiliary task. AuxPPO optimizes θ and θ'

simultaneously by considering the following joint loss

$$L(\theta, \theta') \doteq \sum_{t=0}^{\infty} \gamma^t L_t(\theta, \theta_{\text{old}}) + (1 - \gamma^t) L_t(\theta', \theta_{\text{old}}),$$

where S_t and A_t are obtained by executing θ_{old} . We additionally synchronize θ' with θ periodically to avoid an off-policy learning issue.

Flipped rewards: Besides AuxPPO, we also design novel environments with flipped rewards to investigate Hypothesis 2. Recall we include the time step in the state, this allows us to simply create a new environment by defining a new reward function $r'(s, t) \doteq r(s) \mathbb{I}_{t \leq t_0} - r(s) \mathbb{I}_{t > t_0}$, where \mathbb{I} is the indicator function. During an episode, within the first t_0 steps, this new environment is the same as the original one. After t_0 steps, the sign of the reward is flipped. We select t_0 such that γ^{t_0} is sufficiently small, e.g., we define $t_0 \doteq \min_t \{\gamma^t < 0.05\}$. With this criterion for selecting t_0 , the later transitions (i.e., transitions after t_0 steps) have little influence on the evaluation objective, the discounted return. Consequently, the later transitions affect the overall learning process mainly through representation learning. DisPPO rarely makes use of the later transitions due to the γ_A^t term in the gradient update. AuxPPO makes use of the later transitions only through representation learning. PPO exploits the later transitions for representation learning and the later transitions also affect the control policy of PPO directly.

Results: When we consider the original environments, Fig-

ure 11 shows that in 8 out of 12 tasks, PPO outperforms DisPPO, even if the performance metric is the *discounted* episodic return. In all those 8 tasks, by using the difference term as an auxiliary task, AuxPPO is able to improve upon DisPPO. In 6 out of those 8 tasks, AuxPPO is able to roughly match the performance of PPO at the end of training. For $\gamma \in \{0.93, 0.9\}$ in Ant , the improvement of AuxPPO is not clear and we conjecture that this is because the learning of the π -head (the control head) in AuxPPO is much slower than the learning of π in PPO due to the γ_C^t term. Overall, this suggests that the benefit of PPO over DisPPO comes mainly from representation learning.

When we consider the environments with flipped rewards, PPO is outperformed by DisPPO and AuxPPO by a large margin in 11 out of 12 tasks. The transitions after t_0 steps are not directly relevant when the performance metric is the discounted return. However, learning on those transitions may still improve representation learning provided that those transitions are similar to the earlier transitions, which is the case in the original environments. PPO and AuxPPO, therefore, outperform DisPPO. However, when those transitions are much different from the earlier transitions, which is the case in the environments with flipped rewards, updating the control policy π_θ directly based on those transitions becomes distracting. PPO, therefore, is outperformed by DisPPO. Different from PPO, AuxPPO does not update the control policy π_θ on later transitions directly. Provided that the network has enough capacity, the control policy π_θ in AuxPPO will not be affected much by the irrelevant transitions. The performance of AuxPPO is, therefore, similar to DisPPO.

To summarize, Figure 11 suggests that using $\gamma_A = 1$ is simply an *inductive bias* that *all transitions are equally important*. When this inductive bias is helpful for learning, $\gamma_A = 1$ implicitly implements auxiliary tasks thus improving representation learning and the overall performance. When this inductive bias is detrimental, however, $\gamma_A = 1$ can lead to significant performance drops. AuxPPO appears to be a safe choice that does not depend much on the correctness of this inductive bias.

5. Related Work

The mismatch in actor-critic algorithm implementations has been previously studied. Thomas (2014) focuses on the natural policy gradient setting and shows that the biased implementation ignoring γ_A^t can be interpreted as the gradient of the average reward objective under a strong assumption that the state distribution is independent of the policy. Nota & Thomas (2020) prove that without this strong assumption, the biased implementation is *not* the gradient of any *stationary* objective. This does not contradict our auxiliary task perspective as our objective $J_{s,\mu}(\pi)$ changes at every

time step. Nota & Thomas (2020) further provide a counterexample showing that following the biased gradient can lead to a poorly performing policy w.r.t. both discounted and undiscounted objectives. Both Thomas (2014) and Nota & Thomas (2020), however, focus on *theoretical disadvantages* of the biased gradient and regard ignoring γ_A^t as the source of the bias. We instead regard the introduction of $\gamma_C < 1$ in the critic as the source of the bias in the undiscounted setting and investigate its *empirical advantages*, which are more relevant to practitioners. Moreover, our representation learning perspective for investigating this mismatch is to our knowledge novel.

Although we propose the *bias-variance-representation* trade-off, we do not claim that is all that γ affects. The discount factor also has many other effects (e.g., Sutton (1995); Jiang et al. (2016); Laroché et al. (2017); Laroché & van Seijen (2018); Lehnert et al. (2018); Fedus et al. (2019); Van Seijen et al. (2019); Amit et al. (2020)), the analysis of which we leave for future work. In Scenario 1, using $\gamma_C < 1$ helps reduce the variance. Variance reduction in RL itself is an active research area (see, e.g., Papini et al. (2018); Xu et al. (2019); Yuan et al. (2020)). Investigating those variance reduction techniques with $\gamma_C = 1$ is another possibility for future work. Recently, Bengio et al. (2020) study the effect of the bootstrapping parameter λ in TD(λ) in generalization. Our work studies the effect of the discount factor γ in representation learning in the context of the misuse of the discounting in actor-critic algorithms, sharing a similar spirit of Bengio et al. (2020).

6. Conclusion

In this paper, we investigate the longstanding mismatch between theorists and practitioners in actor-critic algorithms from a representation learning perspective. Although the theoretical understanding of policy gradient algorithms have recently been significantly advanced (Agarwal et al., 2019; Wu et al., 2020), this mismatch has drawn little attention. In this paper, we propose to understand this mismatch from a bias-representation trade-off perspective and an auxiliary task perspective for two different scenarios respectively. We hope our empirical study can help practitioners understand actor-critic algorithms better and therefore design more efficient actor-critic algorithms in the setting of deep RL, where representation learning emerges as a major consideration. We hope our empirical study can draw more attention to the mismatch, which could enable the community to finally close this longstanding gap.

Acknowledgements

We thank Geoffrey J. Gordon, Marc-Alexandre Cote, Bei Peng, and Dipendra Misra for the insightful discussion.

Part of this work was done during SZ’s internship at Microsoft Research Montreal. SZ is also funded by the Engineering and Physical Sciences Research Council (EPSRC). This project has received funding from the European Research Council under the European Union’s Horizon 2020 research and innovation programme (grant agreement number 637713). Part of the experiments was made possible by a generous equipment grant from NVIDIA.

References

- Achiam, J. Spinning up in deep reinforcement learning. 2018.
- Agarwal, A., Kakade, S. M., Lee, J. D., and Mahajan, G. Optimality and approximation with policy gradient methods in markov decision processes. *arXiv preprint arXiv:1908.00261*, 2019.
- Amit, R., Meir, R., and Ciosek, K. Discount factor as a regularizer in reinforcement learning. *arXiv preprint arXiv:2007.02040*, 2020.
- Andrychowicz, M., Raichuk, A., Stańczyk, P., Orsini, M., Girgin, S., Marinier, R., Hussenot, L., Geist, M., Pietquin, O., Michalski, M., et al. What matters in on-policy reinforcement learning? a large-scale empirical study. *arXiv preprint arXiv:2006.05990*, 2020.
- Bellemare, M. G., Naddaf, Y., Veness, J., and Bowling, M. The arcade learning environment: An evaluation platform for general agents. *Journal of Artificial Intelligence Research*, 47:253–279, jun 2013.
- Bellemare, M. G., Dabney, W., and Munos, R. A distributional perspective on reinforcement learning. *arXiv preprint arXiv:1707.06887*, 2017.
- Bengio, E., Pineau, J., and Precup, D. Interference and generalization in temporal difference learning. *arXiv preprint arXiv:2003.06350*, 2020.
- Bertsekas, D. P. and Tsitsiklis, J. N. *Neuro-Dynamic Programming*. Athena Scientific Belmont, MA, 1996.
- Brockman, G., Cheung, V., Pettersson, L., Schneider, J., Schulman, J., Tang, J., and Zaremba, W. Openai gym. *arXiv preprint arXiv:1606.01540*, 2016.
- Caspi, I., Leibovich, G., Novik, G., and Endrawis, S. Reinforcement learning coach, December 2017. URL <https://doi.org/10.5281/zenodo.1134899>.
- Chung, W., Nath, S., Joseph, A., and White, M. Two-timescale networks for nonlinear value function approximation. In *International Conference on Learning Representations*, 2018.
- De Asis, K., Chan, A., Pitis, S., Sutton, R. S., and Graves, D. Fixed-horizon temporal difference methods for stable reinforcement learning. *arXiv preprint arXiv:1909.03906*, 2019.
- Dhariwal, P., Hesse, C., Klimov, O., Nichol, A., Plappert, M., Radford, A., Schulman, J., Sidor, S., Wu, Y., and Zhokhov, P. Openai baselines. <https://github.com/openai/baselines>, 2017.
- Engstrom, L., Ilyas, A., Santurkar, S., Tsipras, D., Janoos, F., Rudolph, L., and Madry, A. Implementation matters in deep rl: A case study on ppo and trpo. In *International Conference on Learning Representations*, 2019.
- Fedus, W., Gelada, C., Bengio, Y., Bellemare, M. G., and Larochelle, H. Hyperbolic discounting and learning over multiple horizons. *arXiv preprint arXiv:1902.06865*, 2019.
- Fujimoto, S., van Hoof, H., and Meger, D. Addressing function approximation error in actor-critic methods. *arXiv preprint arXiv:1802.09477*, 2018.
- Haarnoja, T., Zhou, A., Abbeel, P., and Levine, S. Soft actor-critic: Off-policy maximum entropy deep reinforcement learning with a stochastic actor. *arXiv preprint arXiv:1801.01290*, 2018.
- Henderson, P., Islam, R., Bachman, P., Pineau, J., Precup, D., and Meger, D. Deep reinforcement learning that matters. *arXiv preprint arXiv:1709.06560*, 2017.
- Ilyas, A., Engstrom, L., Santurkar, S., Tsipras, D., Janoos, F., Rudolph, L., and Madry, A. A closer look at deep policy gradients. *arXiv preprint arXiv:1811.02553*, 2018.
- Jaderberg, M., Mnih, V., Czarnecki, W. M., Schaul, T., Leibo, J. Z., Silver, D., and Kavukcuoglu, K. Reinforcement learning with unsupervised auxiliary tasks. *arXiv preprint arXiv:1611.05397*, 2016.
- Jiang, N., Singh, S. P., and Tewari, A. On structural properties of mdps that bound loss due to shallow planning. In *IJCAI*, 2016.
- Kingma, D. P. and Ba, J. Adam: A method for stochastic optimization. *arXiv preprint arXiv:1412.6980*, 2014.
- Konda, V. R. *Actor-critic algorithms*. PhD thesis, Massachusetts Institute of Technology, 2002.
- Kostrikov, I. Pytorch implementations of reinforcement learning algorithms. <https://github.com/ikostrikov/pytorch-a2c-ppo-acktr-gail>, 2018.
- Laroché, R. and van Seijen, H. In reinforcement learning, all objective functions are not equal. 2018.

- Laroche, R., Fatemi, M., Romoff, J., and van Seijen, H. Multi-advisor reinforcement learning. *arXiv preprint arXiv:1704.00756*, 2017.
- Lehnert, L., Laroche, R., and van Seijen, H. On value function representation of long horizon problems. In *AAAI Conference on Artificial Intelligence*, 2018.
- Liang, E., Liaw, R., Nishihara, R., Moritz, P., Fox, R., Goldberg, K., Gonzalez, J., Jordan, M., and Stoica, I. Rllib: Abstractions for distributed reinforcement learning. In *International Conference on Machine Learning*, 2018.
- McCallum, R. *Reinforcement learning with selective perception and hidden state*. PhD thesis, 1997.
- Mnih, V., Badia, A. P., Mirza, M., Graves, A., Lillicrap, T., Harley, T., Silver, D., and Kavukcuoglu, K. Asynchronous methods for deep reinforcement learning. In *Proceedings of the 33rd International Conference on Machine Learning*, 2016.
- Munos, R. Distributional reinforcement learning. Invited talk at European Workshop on Reinforcement Learning https://ewrl.files.wordpress.com/2018/10/distributional_rl.pdf, 2018.
- Nota, C. and Thomas, P. S. Is the policy gradient a gradient? In *Proceedings of the 19th International Conference on Autonomous Agents and Multiagent Systems*, 2020.
- OpenAI. Openai five. <https://openai.com/five/>, 2018.
- Papini, M., Binaghi, D., Canonaco, G., Pirota, M., and Restelli, M. Stochastic variance-reduced policy gradient. *arXiv preprint arXiv:1806.05618*, 2018.
- Pardo, F., Tavakoli, A., Levdi, V., and Kormushev, P. Time limits in reinforcement learning. In *International Conference on Machine Learning*, 2018.
- Petroski Such, F., Madhavan, V., Liu, R., Wang, R., Castro, P. S., Li, Y., Zhi, J., Schubert, L., Bellemare, M. G., Clune, J., and et al. An atari model zoo for analyzing, visualizing, and comparing deep reinforcement learning agents. *Proceedings of the Twenty-Eighth International Joint Conference on Artificial Intelligence*, Aug 2019. doi: 10.24963/ijcai.2019/452. URL <http://dx.doi.org/10.24963/ijcai.2019/452>.
- Romoff, J., Henderson, P., Touati, A., Brunskill, E., Pineau, J., and Ollivier, Y. Separating value functions across time-scales. *arXiv preprint arXiv:1902.01883*, 2019.
- Schulman, J., Levine, S., Abbeel, P., Jordan, M., and Moritz, P. Trust region policy optimization. In *Proceedings of the 32nd International Conference on Machine Learning*, 2015a.
- Schulman, J., Moritz, P., Levine, S., Jordan, M., and Abbeel, P. High-dimensional continuous control using generalized advantage estimation. *arXiv preprint arXiv:1506.02438*, 2015b.
- Schulman, J., Wolski, F., Dhariwal, P., Radford, A., and Klimov, O. Proximal policy optimization algorithms. *arXiv preprint arXiv:1707.06347*, 2017.
- Silver, D., Huang, A., Maddison, C. J., Guez, A., Sifre, L., Van Den Driessche, G., Schrittwieser, J., Antonoglou, I., Panneershelvam, V., Lanctot, M., et al. Mastering the game of go with deep neural networks and tree search. *Nature*, 2016.
- Stooke, A. and Abbeel, P. rlpyt: A research code base for deep reinforcement learning in pytorch. *arXiv preprint arXiv:1909.01500*, 2019.
- Sutton, R. S. Learning to predict by the methods of temporal differences. *Machine Learning*, 1988.
- Sutton, R. S. Td models: Modeling the world at a mixture of time scales. In *Machine Learning Proceedings 1995*. Elsevier, 1995.
- Sutton, R. S. and Barto, A. G. *Reinforcement Learning: An Introduction (2nd Edition)*. MIT press, 2018.
- Sutton, R. S., McAllester, D. A., Singh, S. P., and Mansour, Y. Policy gradient methods for reinforcement learning with function approximation. In *Advances in Neural Information Processing Systems*, 2000.
- Thomas, P. Bias in natural actor-critic algorithms. In *Proceedings of the 31st International Conference on Machine Learning*, 2014.
- Van Seijen, H., Fatemi, M., and Tavakoli, A. Using a logarithmic mapping to enable lower discount factors in reinforcement learning. In *Advances in Neural Information Processing Systems*, 2019.
- Veeriah, V., Hessel, M., Xu, Z., Rajendran, J., Lewis, R. L., Oh, J., van Hasselt, H. P., Silver, D., and Singh, S. Discovery of useful questions as auxiliary tasks. In *Advances in Neural Information Processing Systems*, 2019.
- Veinott, A. F. Discrete dynamic programming with sensitive discount optimality criteria. *The Annals of Mathematical Statistics*, 1969.
- Weitzman, M. L. Gamma discounting. *American Economic Review*, 2001.
- Williams, R. J. Simple statistical gradient-following algorithms for connectionist reinforcement learning. *Machine learning*, 1992.

Wu, Y., Zhang, W., Xu, P., and Gu, Q. A finite time analysis of two time-scale actor critic methods. *arXiv preprint arXiv:2005.01350*, 2020.

Xu, P., Gao, F., and Gu, Q. Sample efficient policy gradient methods with recursive variance reduction. *arXiv preprint arXiv:1909.08610*, 2019.

Yuan, H., Lian, X., Liu, J., and Zhou, Y. Stochastic recursive momentum for policy gradient methods. *arXiv preprint arXiv:2003.04302*, 2020.

Zhang, S. Modularized implementation of deep rl algorithms in pytorch. <https://github.com/ShangtongZhang/DeepRL>, 2018.

A. Proof of Lemma 2

Proof. The proof is based on Appendix B in [Schulman et al. \(2015a\)](#), where perturbation theory is used to prove the performance improvement bound (Lemma 1). To simplify notation, we use a vector and a function interchangeably, *i.e.*, we also use r and μ_0 to denote the reward vector and the initial distribution vector. $J(\pi)$ and $d_\pi(s)$ are shorthand for $J_\gamma(\pi)$ and $d_\pi^\gamma(s)$ with $\gamma = 1$. All vectors are *column* vectors.

Let \mathcal{S}^+ be the set of states excluding s^∞ , *i.e.*, $\mathcal{S}^+ \doteq \mathcal{S}/\{s^\infty\}$, we define $P_\pi \in \mathbb{R}^{|\mathcal{S}^+| \times |\mathcal{S}^+|}$ such that $P_\pi(s, s') \doteq \sum_a \pi(a|s)p(s'|s, a)$. Let $G \doteq \sum_{t=0}^{\infty} P_\pi^t$. According to standard Markov chain theories, $G(s, s')$ is the expected number of times that s' is visited before s^∞ is hit given $S_0 = s$. $T_{\max} < \infty$ implies that G is well-defined and we have $G = (I - P_\pi)^{-1}$. Moreover, $T_{\max} < \infty$ also implies $\forall s, \sum_{s'} G(s, s') \leq T_{\max}$, *i.e.*, $\|G\|_\infty \leq T_{\max}$. We have $J(\pi) = \mu_0^\top G r$.

Let $G' \doteq (I - P_{\pi'})^{-1}$, we have

$$J(\pi') - J(\pi) = \mu_0^\top (G' - G)r.$$

Let $\Delta \doteq P_{\pi'} - P_\pi$, we have

$$G'^{-1} - G^{-1} = -\Delta,$$

Left multiply by G' and right multiply by G ,

$$\begin{aligned} G - G' &= -G' \Delta G, \\ G' &= G + G' \Delta G \quad (\text{Expanding } G' \text{ in RHS recursively}) \\ &= G + G \Delta G + G' \Delta G \Delta G. \end{aligned}$$

So we have

$$J(\pi') - J(\pi) = \mu_0^\top G \Delta G r + \mu_0^\top G' \Delta G \Delta G r.$$

It is easy to see $\mu_0^\top G = d_\pi^\top$ and $G r = v_\pi$. So

$$\begin{aligned} \mu_0^\top G \Delta G r &= d_\pi^\top \Delta v_\pi \\ &= \sum_s d_\pi(s) \sum_{s'} \left(\sum_a \pi'(a|s)p(s'|s, a) - \sum_a \pi(a|s)p(s'|s, a) \right) v_\pi(s') \\ &= \sum_s d_\pi(s) \sum_a (\pi'(a|s) - \pi(a|s)) \sum_{s'} p(s'|s, a) v_\pi(s') \\ &= \sum_s d_\pi(s) \sum_a (\pi'(a|s) - \pi(a|s)) \left(r(s) + \sum_{s'} p(s'|s, a) v_\pi(s') - v_\pi(s) \right) \\ &\quad (\sum_a (\pi'(a|s) - \pi(a|s)) f(s) = 0 \text{ holds for any } f \text{ that depends only on } s) \\ &= \sum_s d_\pi(s) \sum_a \pi'(a|s) \text{Adv}_\pi(s, a). \end{aligned}$$

$$(\sum_a \pi(a|s) \text{Adv}_\pi(s, a) = 0 \text{ by Bellman equation})$$

We now bound $\mu_0^\top G' \Delta G \Delta G r$. First,

$$\begin{aligned} |(\Delta G r)(s)| &= \left| \sum_{s'} \left(\sum_a \pi'(a|s) - \pi(a|s) \right) p(s'|s, a) v_\pi(s') \right| \\ &= \left| \sum_a \left(\pi'(a|s) - \pi(a|s) \right) \left(r(s) + \sum_{s'} p(s'|s, a) v_\pi(s') - v_\pi(s) \right) \right| \\ &= \left| \sum_a \left(\pi'(a|s) - \pi(a|s) \right) \text{Adv}_\pi(s, a) \right| \\ &\leq 2 \max_s D_{TV}(\pi'(\cdot|s), \pi(\cdot|s)) \max_{s,a} |\text{Adv}_\pi(s, a)|, \end{aligned}$$

where D_{TV} is the total variation distance. So

$$\|\Delta Gr\|_\infty \leq 2 \max_s D_{TV}(\pi'(\cdot|s), \pi(\cdot|s)) \max_{s,a} |\text{Adv}_\pi(s, a)|.$$

Moreover, for any vector x ,

$$\begin{aligned} |(\Delta x)(s)| &\leq 2 \max_s D_{TV}(\pi'(\cdot|s), \pi(\cdot|s)) \|x\|_\infty, \\ \|\Delta x\|_\infty &\leq 2 \max_s D_{TV}(\pi'(\cdot|s), \pi(\cdot|s)) \|x\|_\infty. \end{aligned}$$

So

$$\begin{aligned} \|\Delta\|_\infty &\leq 2 \max_s D_{TV}(\pi'(\cdot|s), \pi(\cdot|s)), \\ |\mu_0^\top G' \Delta G \Delta Gr| &\leq \|\mu_0^\top\|_1 \|G'\|_\infty \|\Delta\|_\infty \|G\|_\infty \|\Delta Gr\|_\infty \\ &\leq 4T_{\max}^2 \max_s D_{TV}^2(\pi'(\cdot|s), \pi(\cdot|s)) \max_{s,a} |\text{Adv}_\pi(s, a)| \\ &\leq 4T_{\max}^2 \max_s D_{KL}(\pi(\cdot|s) \|\pi'(\cdot|s)) \max_{s,a} |\text{Adv}_\pi(s, a)|, \end{aligned}$$

which completes the proof. \square

Note this perturbation-based proof of Lemma 2 holds only for $r : \mathcal{S} \rightarrow \mathbb{R}$. For $r : \mathcal{S} \times \mathcal{A} \rightarrow \mathbb{R}$, we can turn to the coupling-based proof as [Schulman et al. \(2015a\)](#), which, however, complicates the presentation and deviates from the main purpose of this paper. We, therefore, leave it for future work.

B. Experiment Details

B.1. Methodology

We use `HalfCheetah`, `Walker`, `Hopper`, `Ant`, `Humanoid`, and `HumanoidStandup` as our benchmarks. We exclude other tasks as we find PPO plateaus quickly there. The tasks we consider have a hard time limit of 1000. Following [Pardo et al. \(2018\)](#), we add time step information into the state, *i.e.*, there is an additional scalar $t/1000$ in the observation vector. Following [Achiam \(2018\)](#), we estimate the KL divergence between the current policy θ and the sampling policy θ_{old} when optimizing the loss (3). When the estimated KL divergence is greater than a threshold, we stop updating the actor and update only the critic with current data. We use Adam ([Kingma & Ba, 2014](#)) as the optimizer and perform grid search for the initial learning rates of Adam optimizers. Let α_A and $\alpha_C \doteq \beta \alpha_A$ be the learning rates for the actor and critic respectively. For each algorithmic configuration (*i.e.*, a curve in a figure), we tune $\alpha_A \in \{0.125, 0.25, 0.5, 1, 2\} \times 3 \cdot 10^{-4}$ and $\beta \in \{1, 3\}$ with grid search in `Ant` with 3 independent runs maximizing the average return of the last 100 training episodes. In particular, $\alpha_A = 3 \cdot 10^{-4}$ and $\beta = 3$ is roughly the default learning rates for the PPO implementation in [Achiam \(2018\)](#). We then run this algorithmic configuration with the best α_A and α_C in all tasks. Overall, we find after removing GAE, smaller learning rates are preferred. When we use FHTD, we additionally consider $H \in \{16, 32, 64, 128, 256, 512, 1024\}$ in the grid search. When we use C51, we additionally consider $V_{\max} \in \{20, 40, 80, 160, 320, 640, 1280, 2560, 5120, 10240, 81920, 163840, 327680\}$ in the grid search. We use PPO-TD with $\gamma_C = 0.99$ as an example to study how the best hyperparameter configuration in `Ant` transfers to other games. As shown in Figure 12, the best learning rates of `Ant` ($\alpha_A = 3 \cdot 10^{-4}$ and $\beta = 3$) yields reasonably good performance in all the other games except `Humanoid`. In the paper, we do not draw a conclusion from a single task. So an outlier is unlikely to affect the overall conclusion.

In the discounted setting, we consider only `Ant`, `HalfCheetah` and their variants. For `Walker2d`, `Hopper`, and `Humanoid`, we find the average episode length of all algorithms are smaller than t_0 , *i.e.*, the flipped reward rarely takes effects. For `HumanoidStandup`, the scale of the reward is too large. To summarize, other four environments are not well-suited for the purpose of our empirical study. Moreover, in the discounted setting, we performed the grid search of the learning rates for both `Ant` and `HalfCheetah`.

B.2. Algorithm Details

The pseudocode of all implemented algorithms are provide in Algorithms 1 - 7 with their architectures illustrated in Figure 13. For hyperparameters that are not included in the grid search, we use the same value as [Dhariwal et al. \(2017\)](#); [Achiam \(2018\)](#).

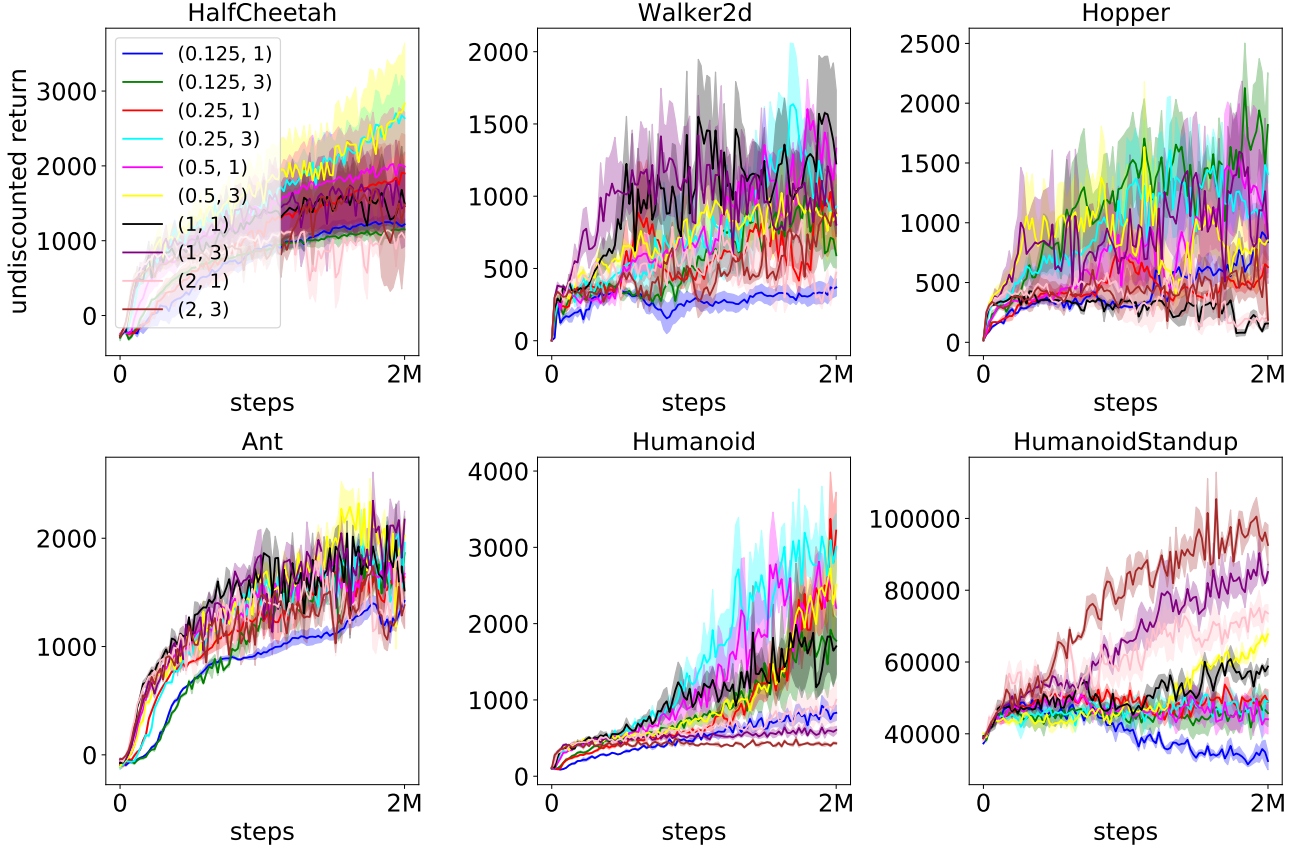


Figure 12: PPO-TD ($\gamma_c = 0.99$) with different learning rates. A curve labeled with (x, β) corresponds to an initial learning rate for the actor and critic of $\alpha_A = x \times 3 \cdot 10^{-4}$ and $\alpha_C = \beta \alpha_A$ respectively. The best learning rates for Ant ($\alpha_A = 3 \cdot 10^{-4}$ and $\beta = 3$) yields reasonably good performance in all the other games except Humanoid.

In particular, for the rollout length, we set $K = 2048$. For the optimization epochs, we set $K_{opt} = 320$. For the minibatch size, we set $B = 64$. For the maximum KL divergence, we set $KL_{target} = 0.01$. We clip $\frac{\pi_{\theta}(a|s)}{\pi_{\theta_{old}}(a|s)}$ into $[-0.2, 0.2]$. We use $N_s = 51$ supports for PPO-C51.

We use two-hidden-layer neural networks for function approximation. Each hidden layer has 64 hidden units and a tanh activation function. The output layer of the actor network has a tanh activation function and is interpreted as the mean of an isotropic Gaussian distribution, whose standard derivation is a global state-independent variable as suggested by Schulman et al. (2015a).

Algorithm 1: PPO

Input:
 θ, ψ : parameters of π, \hat{v} ;

 α_A, α_C : Initial learning rates of the Adam optimizers for θ, ψ ;

 K, K_{opt}, B : rollout length, number of optimization epochs, and minibatch size;

 KL_{target} : maximum KL divergence threshold

;

 $S_0 \sim \mu_0$
while True do

 Initialize a buffer M ;

 $\theta_{old} \leftarrow \theta$;

 for $i = 0, \dots, K - 1$ **do**

 $A_i \sim \pi_{\theta_{old}}(\cdot | S_i)$;

 Execute A_i , get R_{i+1}, S_{i+1} ;

 if S_{i+1} is a terminal state **then**

 $m_i \leftarrow 0, S_{i+1} \sim \mu_0$

 else

 $m_i \leftarrow 1$

 end

 end

 $G_K \leftarrow \hat{v}(S_K)$;

 for $i = K - 1, \dots, 0$ **do**

 $G_i \leftarrow R_{i+1} + \gamma_C m_i G_{i+1}$;

 $\text{Adv}_i \leftarrow R_{i+1} + \gamma_C m_i \hat{v}_\psi(S_{i+1}) - \hat{v}_\psi(S_i)$;

 Store $(S_i, A_i, G_i, \text{Adv}_i)$ in M ;

 end

 Normalize Adv_i in M as $\text{Adv}_i \leftarrow \frac{\text{Adv}_i - \text{mean}(\{\text{Adv}_i\})}{\text{std}(\{\text{Adv}_i\})}$;

 for $o = 1, \dots, K_{opt}$ **do**

 Sample a minibatch $\{(S_i, A_i, G_i, \text{Adv}_i)\}_{i=1, \dots, B}$ from M ;

 $L(\psi) \leftarrow \frac{1}{2B} \sum_{i=1}^B (\hat{v}_\psi(S_i) - G_i)^2$ / * No gradient through G_i * /

 $L(\theta) \leftarrow \frac{1}{B} \sum_{i=1}^B \min\{\frac{\pi_\theta(A_i|S_i)}{\pi_{\theta_{old}}(A_i|S_i)} \text{Adv}_i, \text{clip}(\frac{\pi_\theta(A_i|S_i)}{\pi_{\theta_{old}}(A_i|S_i)}) \text{Adv}_i\}$;

 Perform one gradient update to ψ minimizing $L(\psi)$ with Adam;

 if $\frac{1}{B} \sum_{i=1}^B \log \pi_{\theta_{old}}(A_i|S_i) - \log \pi_\theta(A_i|S_i) < KL_{target}$ **then**

 Perform one gradient update to θ maximizing $L(\theta)$ with Adam;

 end

 end
end

Algorithm 2: PPO-TD

Input:

θ, ψ : parameters of π, \hat{v} ;
 α_A, α_C : Initial learning rates of the Adam optimizers for θ, ψ ;
 K, K_{opt}, B : rollout length, number of optimization epochs, and minibatch size;
 KL_{target} : maximum KL divergence threshold
;

$S_0 \sim \mu_0$

while True do

Initialize a buffer M ;

$\theta_{old} \leftarrow \theta$;

for $i = 0, \dots, K - 1$ **do**

$A_i \sim \pi_{\theta_{old}}(\cdot | S_i)$;

Execute A_i , get R_{i+1}, S_{i+1} ;

if S_{i+1} is a terminal state **then**

| $m_i \leftarrow 0, S_{i+1} \sim \mu_0$

else

| $m_i \leftarrow 1$

end

end

for $i = K - 1, \dots, 0$ **do**

$\text{Adv}_i \leftarrow R_{i+1} + \gamma_C m_i \hat{v}_\psi(S_{i+1}) - \hat{v}_\psi(S_i)$;

$S'_i \leftarrow S_{i+1}, r_i \leftarrow R_{i+1}$;

Store $(S_i, A_i, m_i, r_i, S'_i, \text{Adv}_i)$ in M ;

end

Normalize Adv_i in M as $\text{Adv}_i \leftarrow \frac{\text{Adv}_i - \text{mean}(\{\text{Adv}_i\})}{\text{std}(\{\text{Adv}_i\})}$;

for $o = 1, \dots, K_{opt}$ **do**

Sample a minibatch $\{(S_i, A_i, m_i, r_i, S'_i, \text{Adv}_i)\}_{i=1, \dots, B}$ from M ;

$y_i \leftarrow r_i + \gamma_C m_i \hat{v}_\psi(S'_i)$;

$L(\psi) \leftarrow \frac{1}{2B} \sum_{i=1}^B (\hat{v}_\psi(S_i) - y_i)^2$ / * No gradient through y_i * /

$L(\theta) \leftarrow \frac{1}{B} \sum_{i=1}^B \min\{\frac{\pi_\theta(A_i|S_i)}{\pi_{\theta_{old}}(A_i|S_i)} \text{Adv}_i, \text{clip}(\frac{\pi_\theta(A_i|S_i)}{\pi_{\theta_{old}}(A_i|S_i)}) \text{Adv}_i\}$;

Perform one gradient update to ψ minimizing $L(\psi)$ with Adam;

if $\frac{1}{B} \sum_{i=1}^B \log \pi_{\theta_{old}}(A_i|S_i) - \log \pi_\theta(A_i|S_i) < KL_{target}$ **then**

| Perform one gradient update to θ maximizing $L(\theta)$ with Adam;

end

end

end

Algorithm 3: PPO-TD-Ex
Input:

θ, ψ : parameters of π, \hat{v} ;
 α_A, α_C : Initial learning rates of the Adam optimizers for θ, ψ ;
 K, K_{opt}, B : rollout length, number of optimization epochs, and minibatch size;
 KL_{target} : maximum KL divergence threshold ;
 N : number of extra transitions ;
 p, r : transition kernel and reward function of the oracle
 ;
 $S_0 \sim \mu_0$

while True do

Initialize a buffer M ;

$\theta_{old} \leftarrow \theta$;

for $i = 0, \dots, K - 1$ **do**

for $j = 0, \dots, N$ **do**

$A_i^j \sim \pi_{\theta_{old}}(\cdot | S_i), R_{i+1}^j \leftarrow r(S_i, A_i^j), S_{i+1}^j \sim p(\cdot | S_i, A_i^j)$;

if S_{i+1}^j *is a terminal state* **then**

$m_i^j \leftarrow 0, S_{i+1}^j \sim \mu_0$

else

$m_i^j \leftarrow 1$

end

end

$S_{i+1} \leftarrow S_{i+1}^0$

end

for $i = K - 1, \dots, 0$ **do**

$\text{Adv}_i \leftarrow R_{i+1}^0 + \gamma_C m_i^0 \hat{v}_\psi(S_{i+1}^0) - \hat{v}_\psi(S_i^0)$;

for $j = 0, \dots, N$ **do**

$S_i'^j \leftarrow S_{i+1}^j$

end

 Store $(\{S_i^j, A_i^j, m_i^j, r_i^j, S_i'^j\}_{j=0, \dots, N}, \text{Adv}_i)$ in M ;

end

Normalize Adv_i in M as $\text{Adv}_i \leftarrow \frac{\text{Adv}_i - \text{mean}(\{\text{Adv}_i\})}{\text{std}(\{\text{Adv}_i\})}$;

for $o = 1, \dots, K_{opt}$ **do**

 Sample a minibatch $\{(\{S_i^j, A_i^j, m_i^j, r_i^j, S_i'^j\}_{j=0, \dots, N}, \text{Adv}_i)\}_{i=1, \dots, B}$ from M ;

$y_i \leftarrow \frac{1}{N+1} \sum_{j=0}^N r_i^j + \gamma_C m_i^j \hat{v}_\psi(S_i'^j)$;

$L(\psi) \leftarrow \frac{1}{2B} \sum_{i=1}^B (\hat{v}_\psi(S_i^0) - y_i)^2$ * No gradient through y_i * /

$L(\theta) \leftarrow \frac{1}{B} \sum_{i=1}^B \min\{\frac{\pi_\theta(A_i^0 | S_i^0)}{\pi_{\theta_{old}}(A_i^0 | S_i^0)} \text{Adv}_i, \text{clip}(\frac{\pi_\theta(A_i^0 | S_i^0)}{\pi_{\theta_{old}}(A_i^0 | S_i^0)}) \text{Adv}_i\}$;

 Perform one gradient update to ψ minimizing $L(\psi)$ with Adam;

if $\frac{1}{B} \sum_{i=1}^B \log \pi_{\theta_{old}}(A_i^0 | S_i^0) - \log \pi_\theta(A_i^0 | S_i^0) < KL_{target}$ **then**

 Perform one gradient update to θ maximizing $L(\theta)$ with Adam;

end

end

end

Algorithm 4: PPO-FHTD
Input:
 θ, ψ : parameters of $\pi, \{\hat{v}^j\}_{j=1,\dots,H}$;

 α_A, α_C : Initial learning rates of the Adam optimizers for θ, ψ ;

 K, K_{opt}, B : rollout length, number of optimization epochs, and minibatch size;

 KL_{target} : maximum KL divergence threshold

;

 $S_0 \sim \mu_0$
while True do

 Initialize a buffer M ;

 $\theta_{old} \leftarrow \theta$;

for $i = 0, \dots, K - 1$ **do**
 $A_i \sim \pi_{\theta_{old}}(\cdot | S_i)$;

 Execute A_i , get R_{i+1}, S_{i+1} ;

if S_{i+1} *is a terminal state* **then**

 | $m_i \leftarrow 0, S_{i+1} \sim \mu_0$
else

 | $m_i \leftarrow 1$
end
end
for $i = K - 1, \dots, 0$ **do**
 $\text{Adv}_i \leftarrow R_{i+1} + m_i \hat{v}_\psi^H(S_{i+1}) - \hat{v}_\psi^H(S_i)$;

 $S'_i \leftarrow S_{i+1}, r_i \leftarrow R_{i+1}$;

 Store $(S_i, A_i, m_i, r_i, S'_i, \text{Adv}_i)$ in M ;

end

 Normalize Adv_i in M as $\text{Adv}_i \leftarrow \frac{\text{Adv}_i - \text{mean}(\{\text{Adv}_i\})}{\text{std}(\{\text{Adv}_i\})}$;

for $o = 1, \dots, K_{opt}$ **do**

 Sample a minibatch $\{(S_i, A_i, m_i, r_i, S'_i, \text{Adv}_i)\}_{i=1,\dots,B}$ from M ;

for $j = 1, \dots, H$ **do**

 | $y_i^j \leftarrow r_i + m_i \hat{v}_\psi^{j-1}(S'_i)$ $/* \hat{v}^0(S'_i) \equiv 0$
 $*/$
end
 $L(\psi) \leftarrow \frac{1}{2B} \sum_{i=1}^B \sum_{j=1}^H (\hat{v}_\psi^j(S_i) - y_i^j)^2$ $/*$ No gradient through y_i^j
 $*/$
 $L(\theta) \leftarrow \frac{1}{B} \sum_{i=1}^B \min\{\frac{\pi_\theta(A_i|S_i)}{\pi_{\theta_{old}}(A_i|S_i)} \text{Adv}_i, \text{clip}(\frac{\pi_\theta(A_i|S_i)}{\pi_{\theta_{old}}(A_i|S_i)}) \text{Adv}_i\}$;

 Perform one gradient update to ψ minimizing $L(\psi)$ with Adam;

if $\frac{1}{B} \sum_{i=1}^B \log \pi_{\theta_{old}}(A_i|S_i) - \log \pi_\theta(A_i|S_i) < KL_{target}$ **then**

 | Perform one gradient update to θ maximizing $L(\theta)$ with Adam;

end
end
end

Algorithm 5: PPO-C51
Input:

θ, ψ : parameters of $\pi, \{\hat{v}^j\}_{j=1, \dots, N_s}$ with N_s being the number of supports and \hat{v}^j being the probability of each support;

α_A, α_C : Initial learning rates of the Adam optimizers for θ, ψ ;

K, K_{opt}, B : rollout length, number of optimization epochs, and minibatch size;

KL_{target} : maximum KL divergence threshold

;

$\Delta_z \doteq \frac{2V_{\max}}{N_s-1}, \{z_j \doteq -V_{\max} + (j-1)\Delta_z : j = 1, \dots, N_s\}$ // Define the supports

$S_0 \sim \mu_0$

while True do

 Initialize a buffer M ;

$\theta_{old} \leftarrow \theta$;

for $i = 0, \dots, K-1$ **do**

$A_i \sim \pi_{\theta_{old}}(\cdot | S_i)$;

 Execute A_i , get R_{i+1}, S_{i+1} ;

if S_{i+1} is a terminal state **then**

$m_i \leftarrow 0, S_{i+1} \sim \mu_0$

else

$m_i \leftarrow 1$

end

end
for $i = K-1, \dots, 0$ **do**

$\text{Adv}_i \leftarrow R_{i+1} + m_i \gamma_C \sum_{j=1}^{N_s} \hat{v}_{\psi}^j(S_{i+1}) z_j - \sum_{j=1}^{N_s} \hat{v}_{\psi}^j(S_i) z_j$;

$S'_i \leftarrow S_{i+1}, r_i \leftarrow R_{i+1}$;

 Store $(S_i, A_i, m_i, r_i, S'_i, \text{Adv}_i)$ in M ;

end

Normalize Adv_i in M as $\text{Adv}_i \leftarrow \frac{\text{Adv}_i - \text{mean}(\{\text{Adv}_i\})}{\text{std}(\{\text{Adv}_i\})}$;

for $o = 1, \dots, K_{opt}$ **do**

 Sample a minibatch $\{(S_i, A_i, m_i, r_i, S'_i, \text{Adv}_i)\}_{i=1, \dots, B}$ from M ;

for $i = 1, \dots, B$ **do**
for $j = 1, \dots, N_s$ **do**

$z_j^i \leftarrow r_i + m_i \gamma_C z_j$

end
end
for $j = 1, \dots, N_s$ **do**

$y_j^i \leftarrow \sum_{k=1}^{N_s} [1 - \frac{||z_j^i| - V_{\max}^{\max} - z_j^i|}{\Delta_z}]_0^1 \hat{v}_{\psi}^k(S'_i) / * [x]_l^u \doteq \min(\max(x, l), u)$ */

end

$L(\psi) \leftarrow \frac{1}{B} \sum_{i=1}^B \sum_{j=1}^{N_s} -y_j^i \log \hat{v}_{\psi}^j(S_i) / *$ No gradient through y_j^i */

$L(\theta) \leftarrow \frac{1}{B} \sum_{i=1}^B \min\{\frac{\pi_{\theta}(A_i|S_i)}{\pi_{\theta_{old}}(A_i|S_i)} \text{Adv}_i, \text{clip}(\frac{\pi_{\theta}(A_i|S_i)}{\pi_{\theta_{old}}(A_i|S_i)}) \text{Adv}_i\}$;

Perform one gradient update to ψ minimizing $L(\psi)$ with Adam;

if $\frac{1}{B} \sum_{i=1}^B \log \pi_{\theta_{old}}(A_i|S_i) - \log \pi_{\theta}(A_i|S_i) < KL_{target}$ **then**

 Perform one gradient update to θ maximizing $L(\theta)$ with Adam;

end
end
end

Algorithm 6: DisPPO

Input:
 θ, ψ : parameters of π, \hat{v} ;

 α_A, α_C : Initial learning rates of the Adam optimizers for θ, ψ ;

 K, K_{opt}, B : rollout length, number of optimization epochs, and minibatch size;

 KL_{target} : maximum KL divergence threshold

;

 $S_0 \sim \mu_0, t \leftarrow 0$
while True do

 Initialize a buffer M ;

 $\theta_{old} \leftarrow \theta$;

 for $i = 0, \dots, K - 1$ **do**

 $A_i \sim \pi_{\theta_{old}}(\cdot | S_i), t_i \leftarrow t$;

 Execute A_i , get R_{i+1}, S_{i+1} ;

 if S_{i+1} is a terminal state **then**

 $m_i \leftarrow 0, S_{i+1} \sim \mu_0, t \leftarrow 0$

 else

 $m_i \leftarrow 1, t \leftarrow t + 1$

 end

 end

 $G_K \leftarrow \hat{v}(S_K)$;

 for $i = K - 1, \dots, 0$ **do**

 $G_i \leftarrow R_{i+1} + \gamma_C m_i G_{i+1}$;

 $\text{Adv}_i \leftarrow R_{i+1} + \gamma_C m_i \hat{v}_\psi(S_{i+1}) - \hat{v}_\psi(S_i)$;

 Store $(S_i, A_i, G_i, \text{Adv}_i, t_i)$ in M ;

 end

 Normalize Adv_i in M as $\text{Adv}_i \leftarrow \frac{\text{Adv}_i - \text{mean}(\{\text{Adv}_i\})}{\text{std}(\{\text{Adv}_i\})}$;

 for $o = 1, \dots, K_{opt}$ **do**

 Sample a minibatch $\{(S_i, A_i, G_i, \text{Adv}_i, t_i)\}_{i=1, \dots, B}$ from M ;

 $L(\psi) \leftarrow \frac{1}{2B} \sum_{i=1}^B (\hat{v}_\psi(S_i) - G_i)^2$ / * No gradient through G_i * /

 $L(\theta) \leftarrow \frac{1}{B} \sum_{i=1}^B \gamma_A^{t_i} \min\{\frac{\pi_\theta(A_i|S_i)}{\pi_{\theta_{old}}(A_i|S_i)} \text{Adv}_i, \text{clip}(\frac{\pi_\theta(A_i|S_i)}{\pi_{\theta_{old}}(A_i|S_i)}) \text{Adv}_i\}$;

 Perform one gradient update to ψ minimizing $L(\psi)$ with Adam;

 if $\frac{1}{B} \sum_{i=1}^B \log \pi_{\theta_{old}}(A_i|S_i) - \log \pi_\theta(A_i|S_i) < KL_{target}$ **then**

 Perform one gradient update to θ maximizing $L(\theta)$ with Adam;

 end

 end
end

Algorithm 7: AuxPPO

Input:

θ, θ', ψ : parameters of π, π', \hat{v} ;
 α_A, α_C : Initial learning rates of the Adam optimizers for θ, ψ ;
 K, K_{opt}, B : rollout length, number of optimization epochs, and minibatch size;
 KL_{target} : maximum KL divergence threshold
;

$S_0 \sim \mu_0, t \leftarrow 0$
while *True* **do**

Initialize a buffer M ;

$\theta_{old} \leftarrow \theta, \theta' \leftarrow \theta$;

for $i = 0, \dots, K - 1$ **do**

$A_i \sim \pi_{\theta_{old}}(\cdot | S_i), t_i \leftarrow t$;

Execute A_i , get R_{i+1}, S_{i+1} ;

if S_{i+1} *is a terminal state* **then**

| $m_i \leftarrow 0, S_{i+1} \sim \mu_0, t \leftarrow 0$

else

| $m_i \leftarrow 1, t \leftarrow t + 1$

end

end

$G_K \leftarrow \hat{v}(S_K)$;

for $i = K - 1, \dots, 0$ **do**

$G_i \leftarrow R_{i+1} + \gamma_C m_i G_{i+1}$;

$\text{Adv}_i \leftarrow R_{i+1} + \gamma_C m_i \hat{v}_\psi(S_{i+1}) - \hat{v}_\psi(S_i)$;

Store $(S_i, A_i, G_i, \text{Adv}_i, t_i)$ in M ;

end

Normalize Adv_i in M as $\text{Adv}_i \leftarrow \frac{\text{Adv}_i - \text{mean}(\{\text{Adv}_i\})}{\text{std}(\{\text{Adv}_i\})}$;

for $o = 1, \dots, K_{opt}$ **do**

Sample a minibatch $\{(S_i, A_i, G_i, \text{Adv}_i, t_i)\}_{i=1, \dots, B}$ from M ;

$L(\psi) \leftarrow \frac{1}{2B} \sum_{i=1}^B (\hat{v}_\psi(S_i) - G_i)^2$ * No gradient through G_i * /

$$\begin{aligned}
L(\theta, \theta') \leftarrow & \frac{1}{B} \sum_{i=1}^B \gamma_C^{t_i} \min \left\{ \frac{\pi_\theta(A_i | S_i)}{\pi_{\theta_{old}}(A_i | S_i)} \text{Adv}_i, \text{clip} \left(\frac{\pi_\theta(A_i | S_i)}{\pi_{\theta_{old}}(A_i | S_i)} \right) \text{Adv}_i \right\} + \\
& (1 - \gamma_C^{t_i}) \min \left\{ \frac{\pi_{\theta'}(A_i | S_i)}{\pi_{\theta_{old}}(A_i | S_i)} \text{Adv}_i, \text{clip} \left(\frac{\pi_{\theta'}(A_i | S_i)}{\pi_{\theta_{old}}(A_i | S_i)} \right) \text{Adv}_i \right\}
\end{aligned}$$

;

Perform one gradient update to ψ minimizing $L(\psi)$ with Adam;

if $\frac{1}{B} \sum_{i=1}^B \log \pi_{\theta_{old}}(A_i | S_i) - \log \pi_\theta(A_i | S_i) < KL_{target}$ **then**

| Perform one gradient update to θ, θ' maximizing $L(\theta, \theta')$ with Adam;

end

end

end

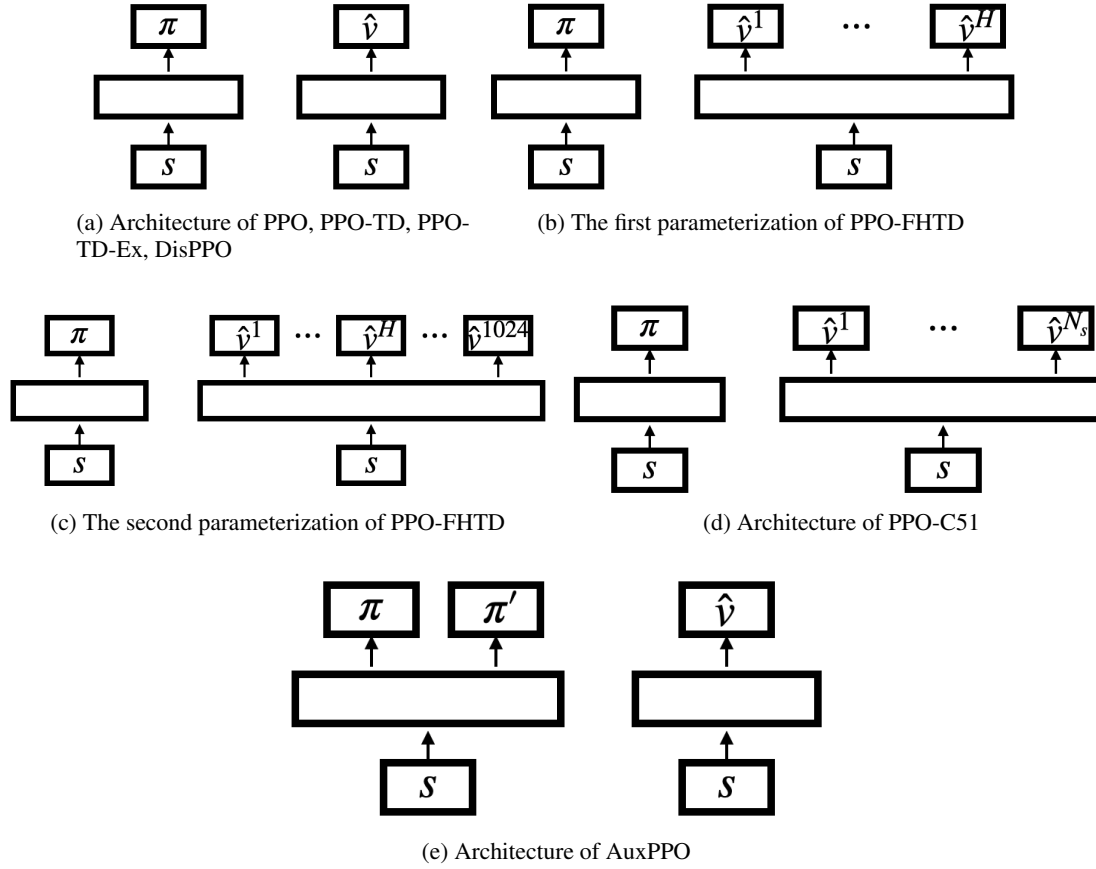


Figure 13: Architectures of the algorithms

C. Additional Experimental Results

C.1. Distributional RL

Hypothesis 1 and the previous empirical study suggest that representation learning may be the main bottleneck of PPO-TD ($\gamma_c = 1$). To further support this, we benchmark PPO-C51 ($\gamma_c = 1$) (Algorithm 5 in the appendix), where the critic of PPO is trained with C51. C51 is usually considered to improve representation learning by implicitly providing auxiliary tasks (Bellemare et al., 2017; Munos, 2018; Petroski Such et al., 2019). Figure 14 shows that training the critic with C51 indeed leads to a performance improvement and PPO-C51 ($\gamma_c = 1$) sometimes outperforms PPO-TD ($\gamma_c < 1$) by a large margin. Figure 15 further shows that when V_{\max} is optimized for PPO-C51, the benefit for using $\gamma_c < 1$ in PPO-C51 is less pronounced than that in PPO-TD, indicating the role of $\gamma_c < 1$ and distributional learning may overlap. Figures 6, 7, & 8, suggest that the overlapping is representation learning.

C.2. Other Complementary Results

Figure 16 shows how PPO-TD-Ex ($\gamma_c = 0.995$) reacts to the increase of N . Figure 17 shows the unnormalized representation error in the MRP experiment. Figure 18 shows the average episode length for the Ant environment in the discounted setting. For HalfCheetah, it is always 1000.

D. Larger Version of Figures

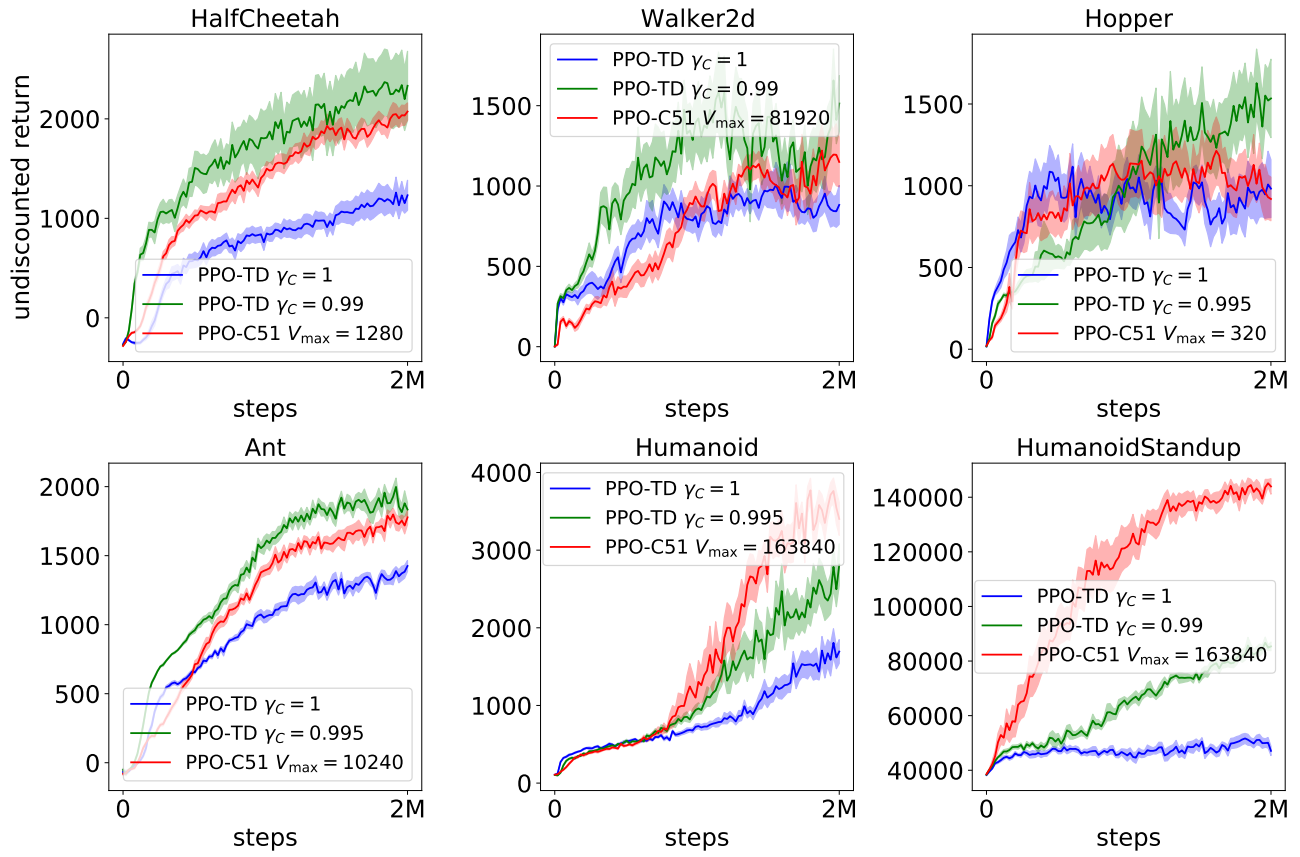


Figure 14: For PPO-C51, we set $\gamma_C = 1$.

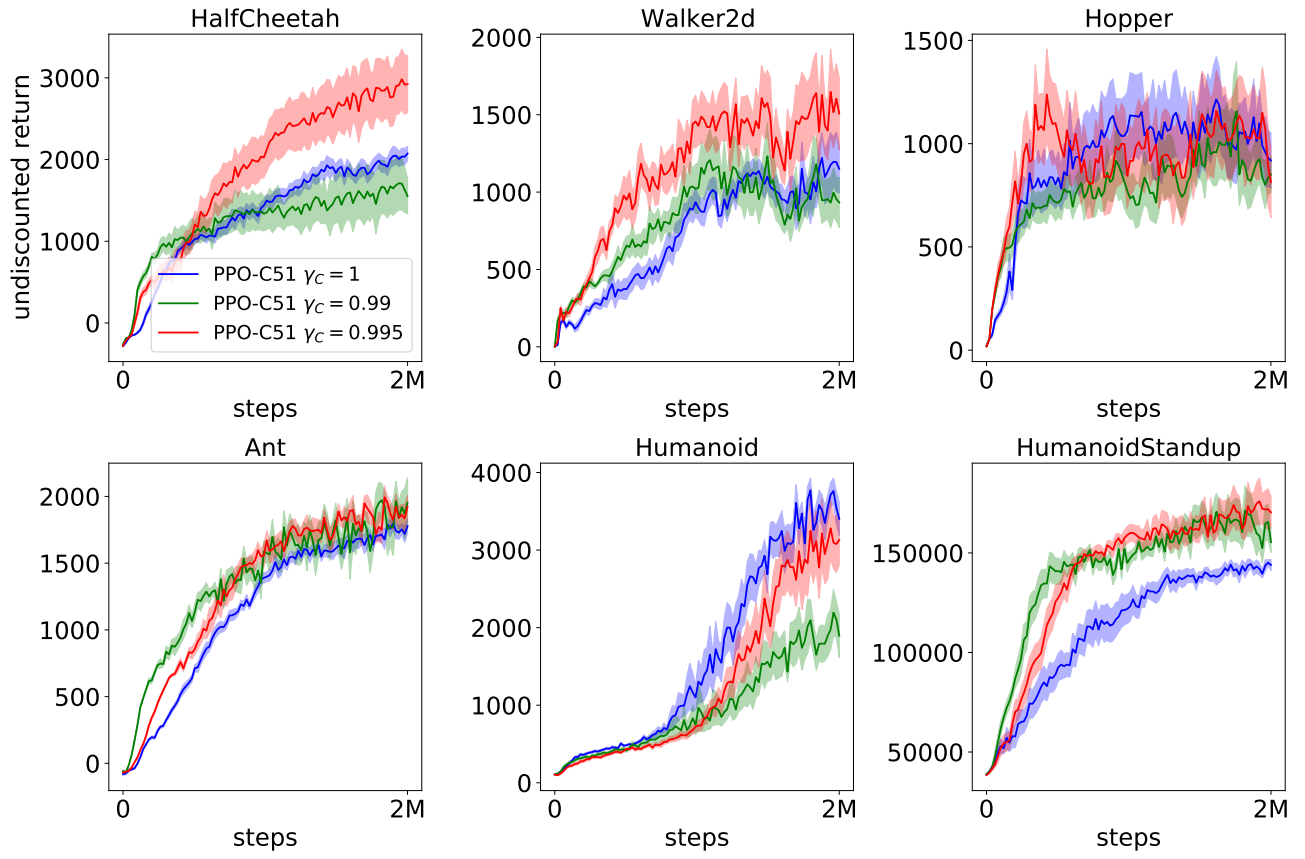


Figure 15: For each game, V_{\max} is the same as the V_{\max} in Figure 14.

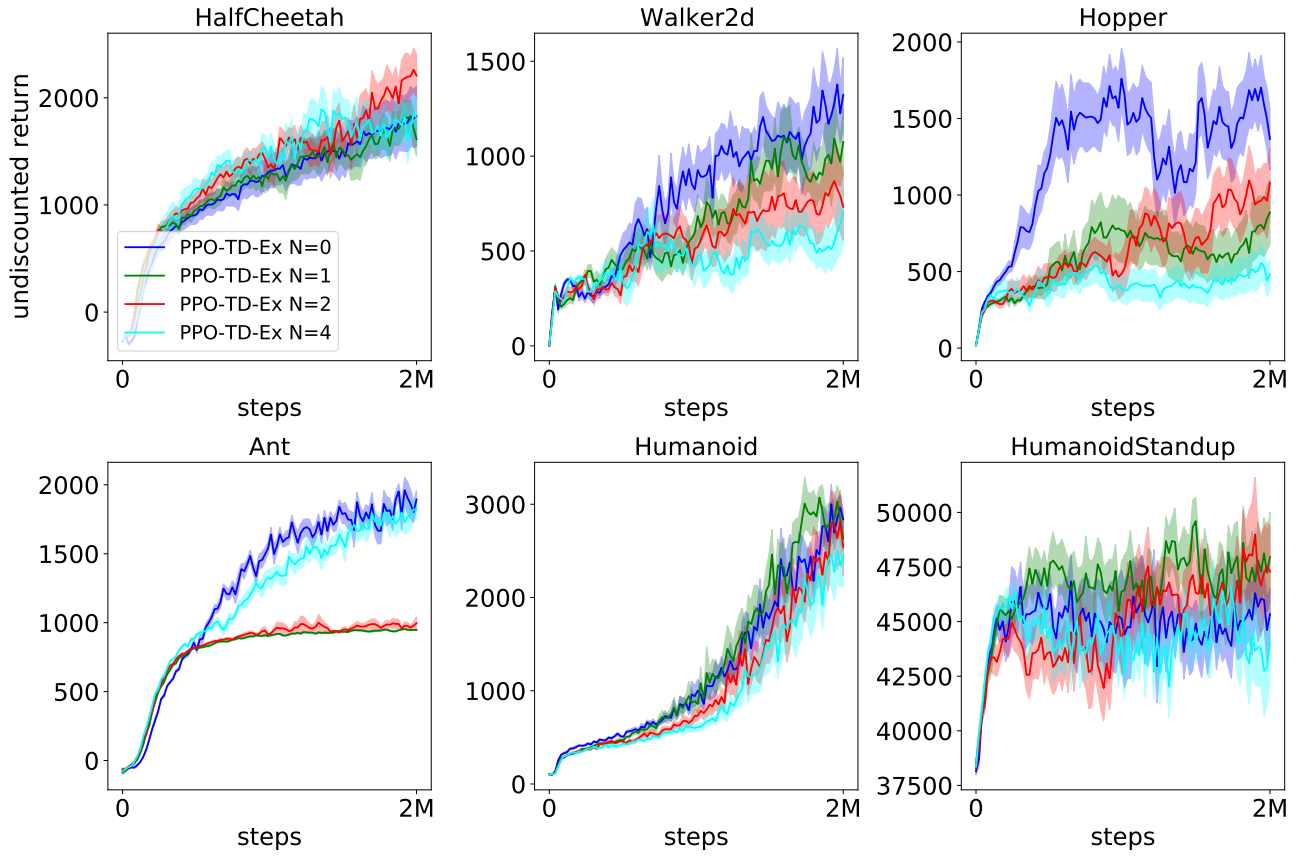


Figure 16: PPO-TD-Ex ($\gamma_c = 0.995$).

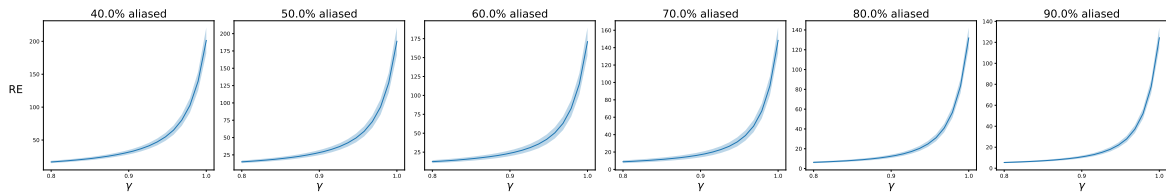


Figure 17: Unnormalized representation error (RE) as a function of the discount factor. Shaded regions indicate one standard deviation. RE is computed analytically as $\text{RE}(X, \gamma) \doteq \min_w \|Xw - v_\gamma\|_2$

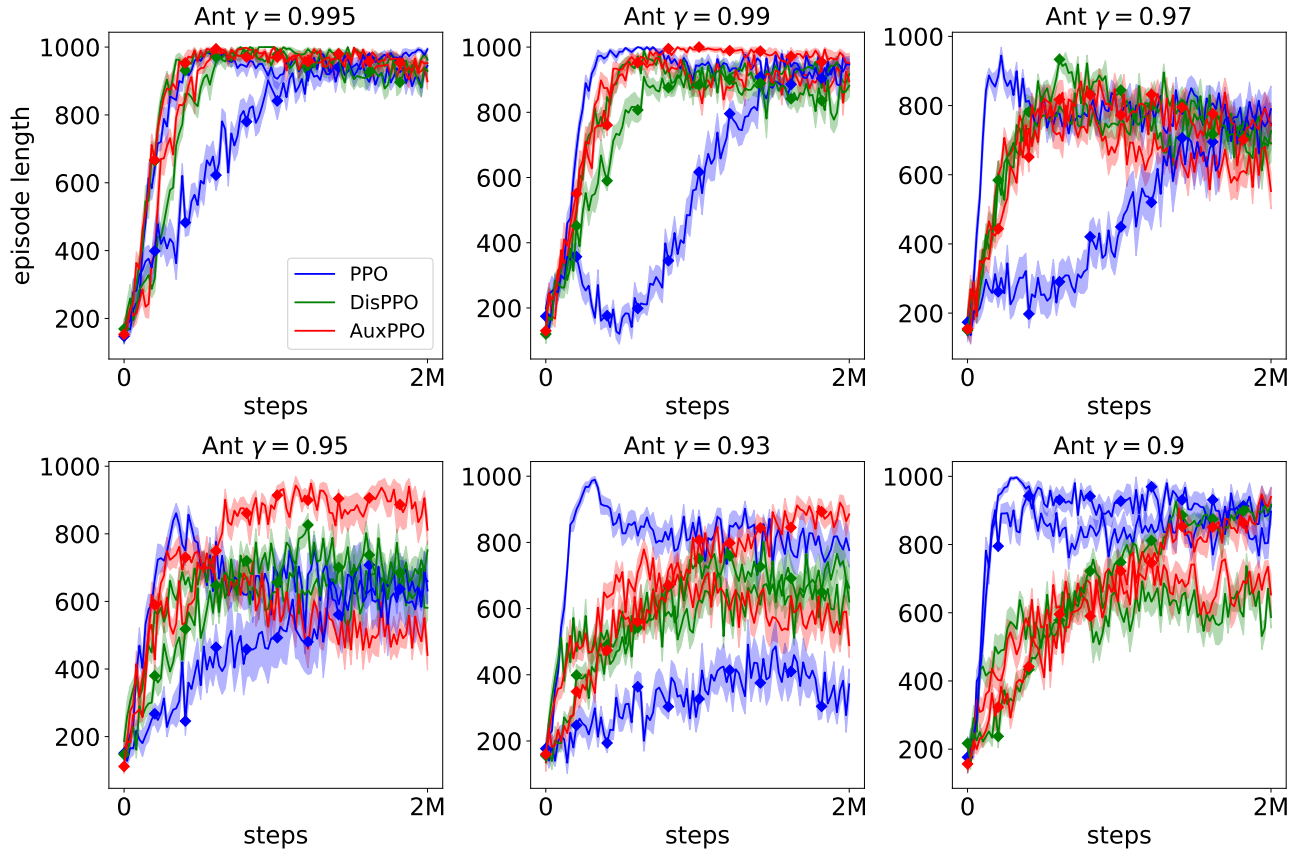


Figure 18: Curves without any marker are obtained in the original Ant. Diamond-marked curves are obtained in Ant with r' .

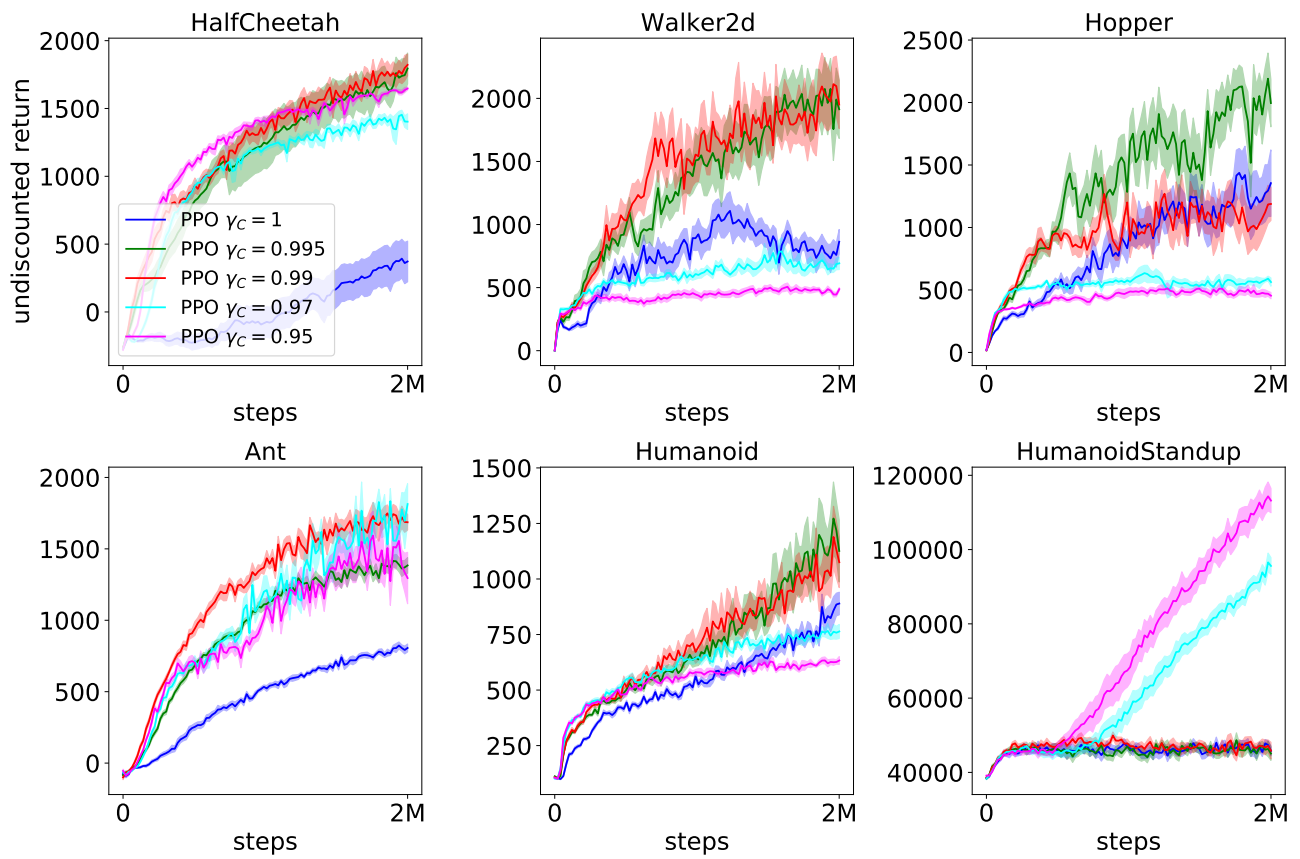


Figure 19: The default PPO implementation with different discount factors. The larger version of Figure 1.

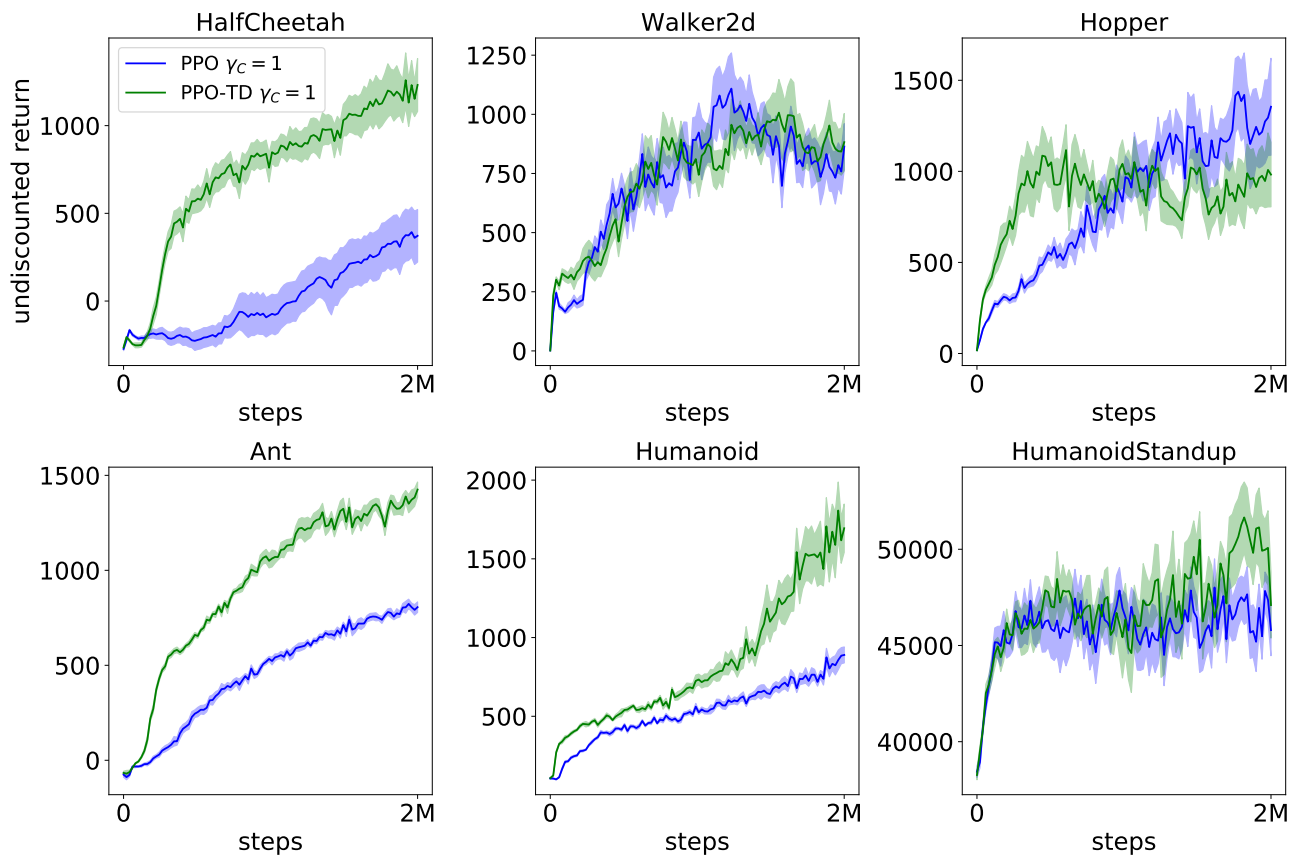


Figure 20: Comparison between PPO and PPO-TD when $\gamma_c = 1$. The larger version of Figure 2.

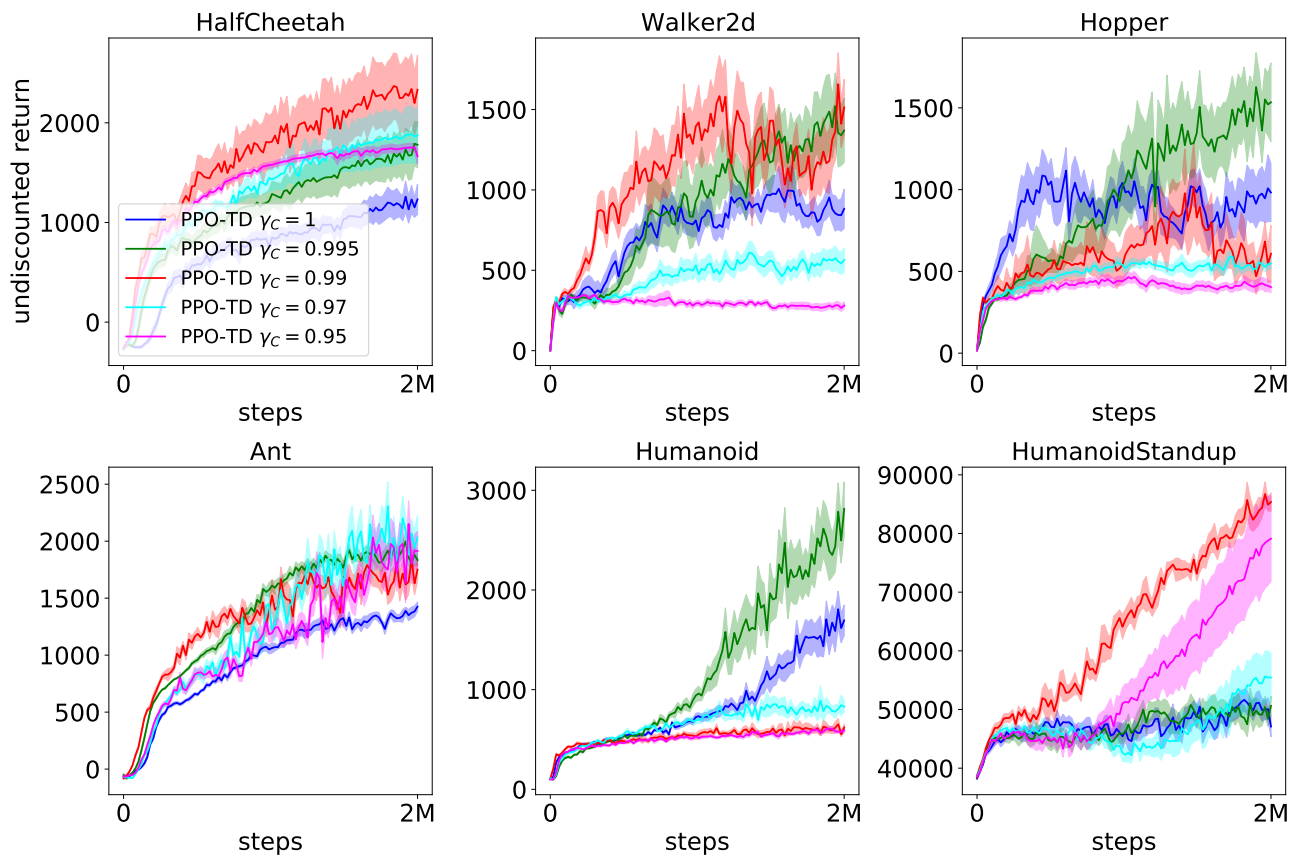


Figure 21: PPO-TD with different discount factors. The larger version of Figure 3.

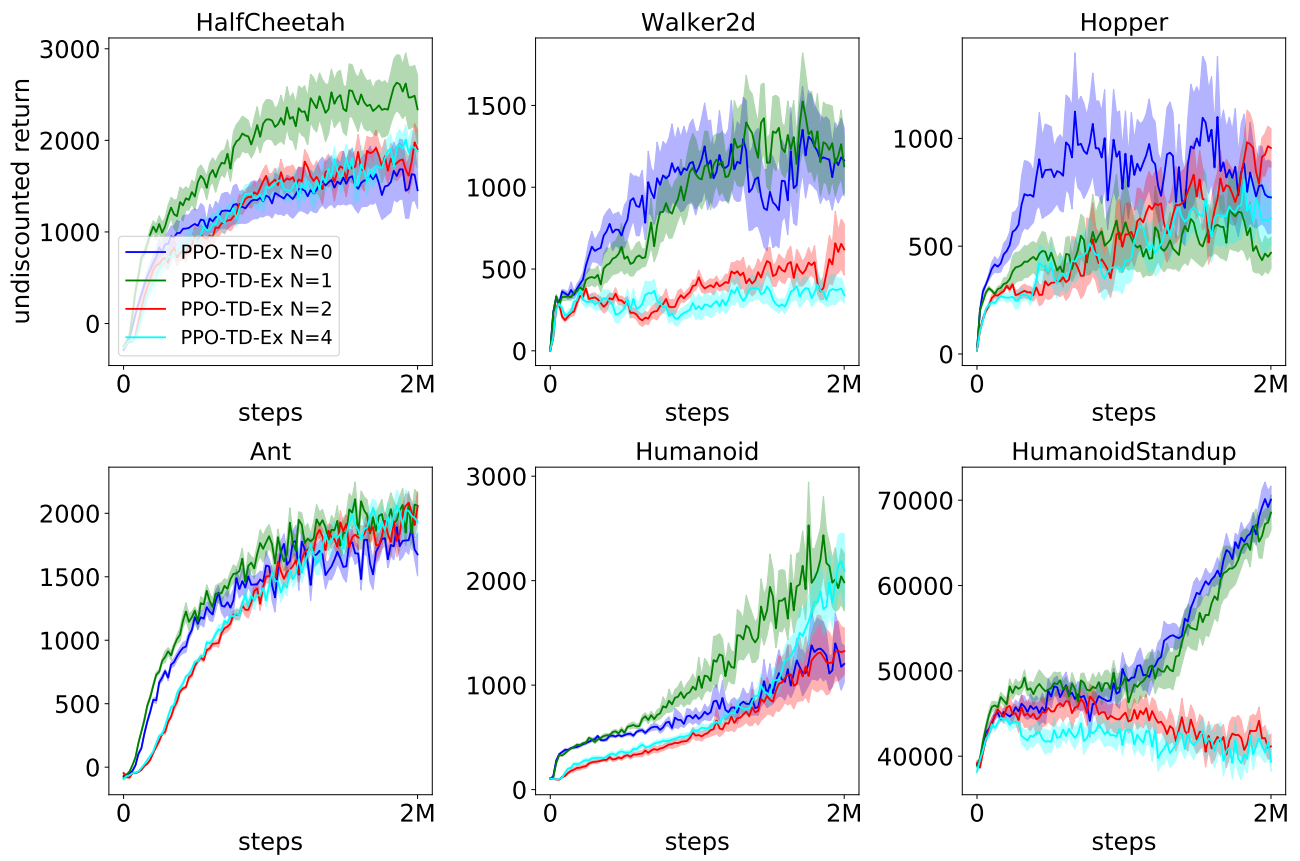


Figure 22: PPO-TD-Ex ($\gamma_c = 0.99$). The larger version of Figure 4.

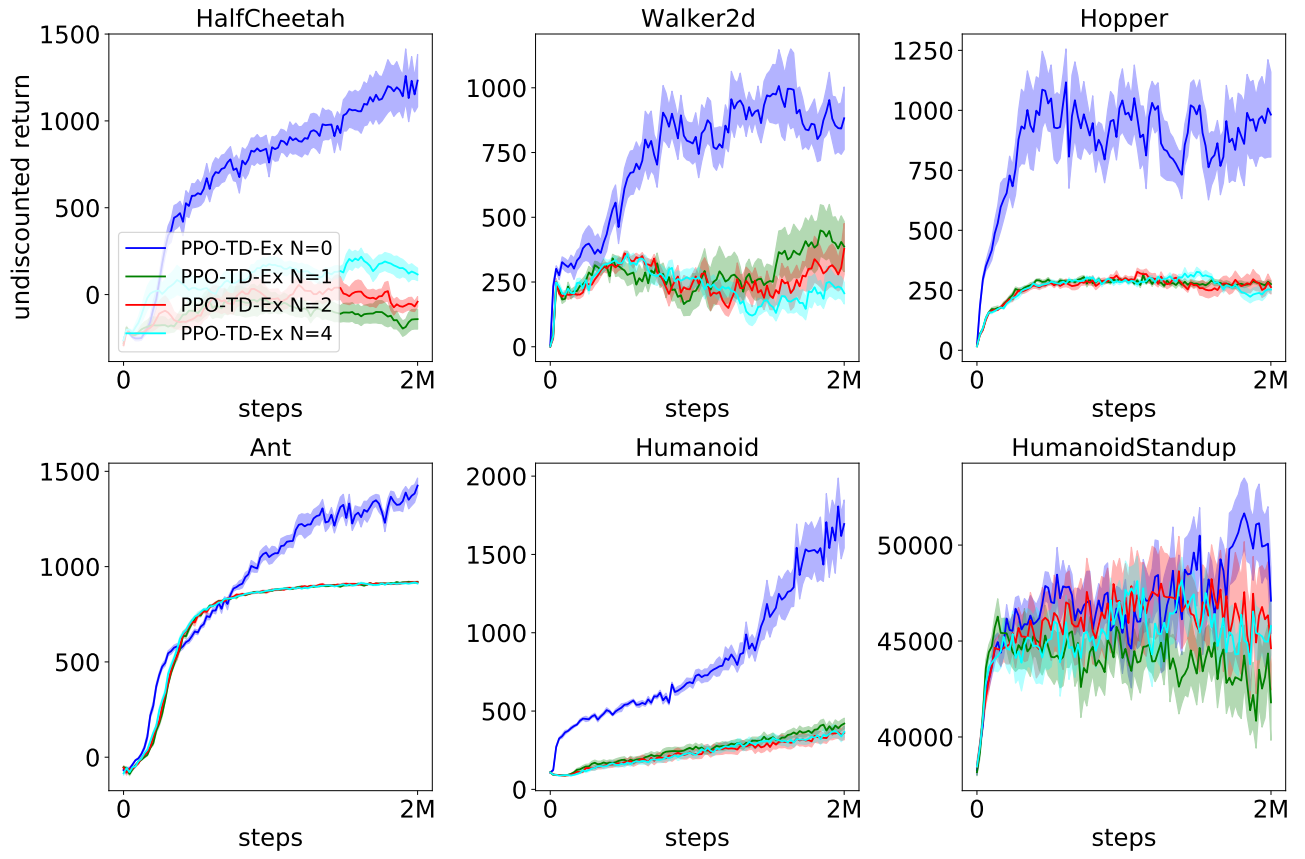


Figure 23: PPO-TD-Ex ($\gamma_c = 1$). The larger version of Figure 5.

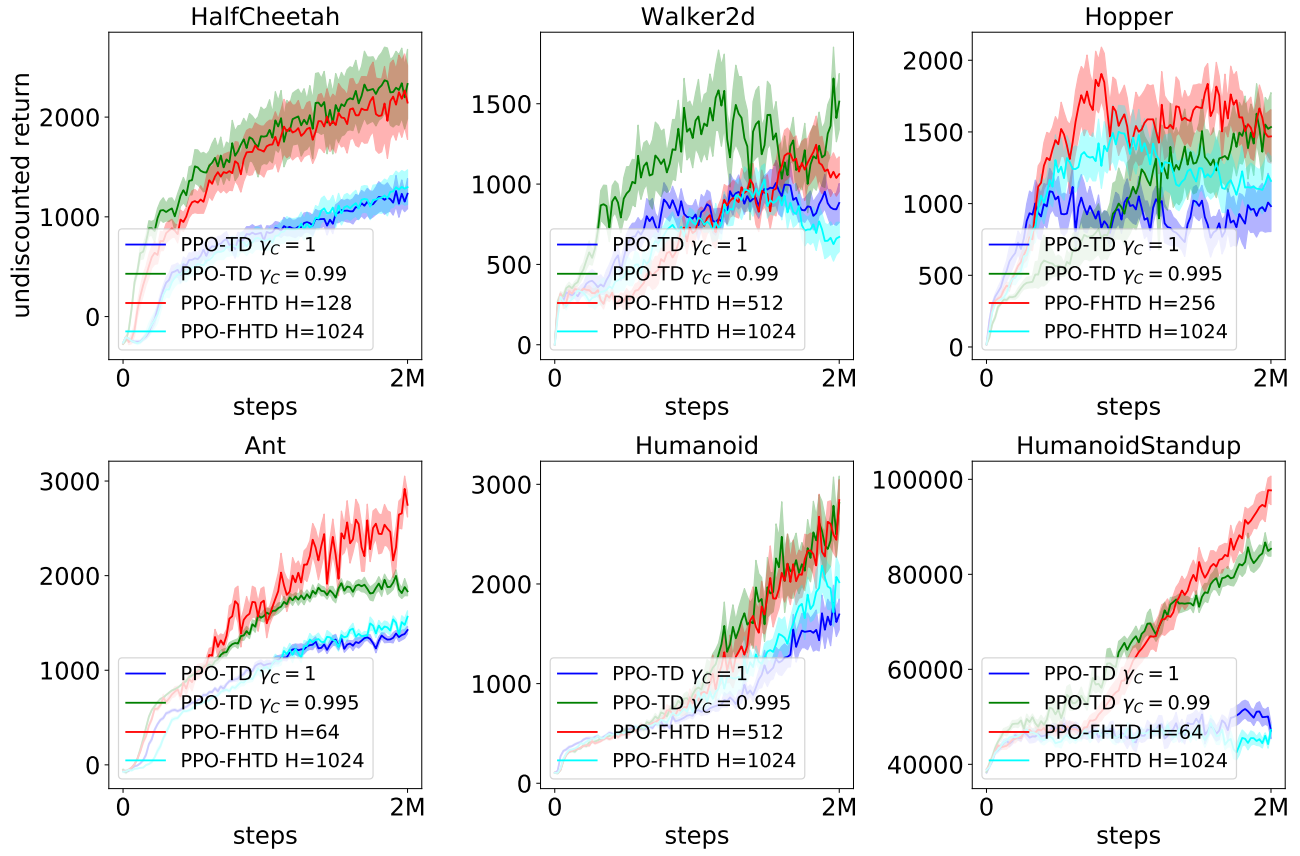


Figure 24: PPO-FHTD with the first parameterization. The best H and γ_c are used for each game. The larger version of Figure 6.

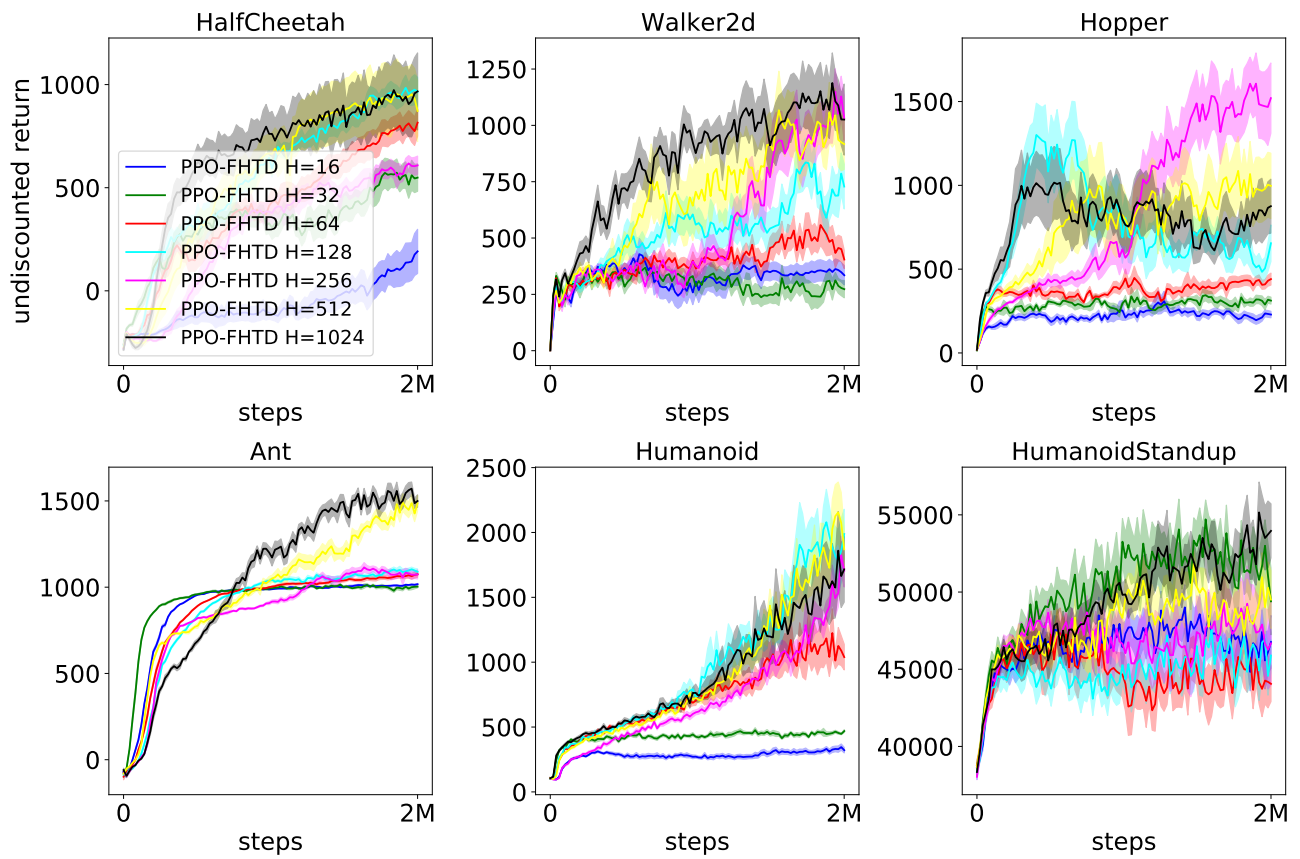


Figure 25: PPO-FHTD with the second parameterization. The larger version of Figure 7.

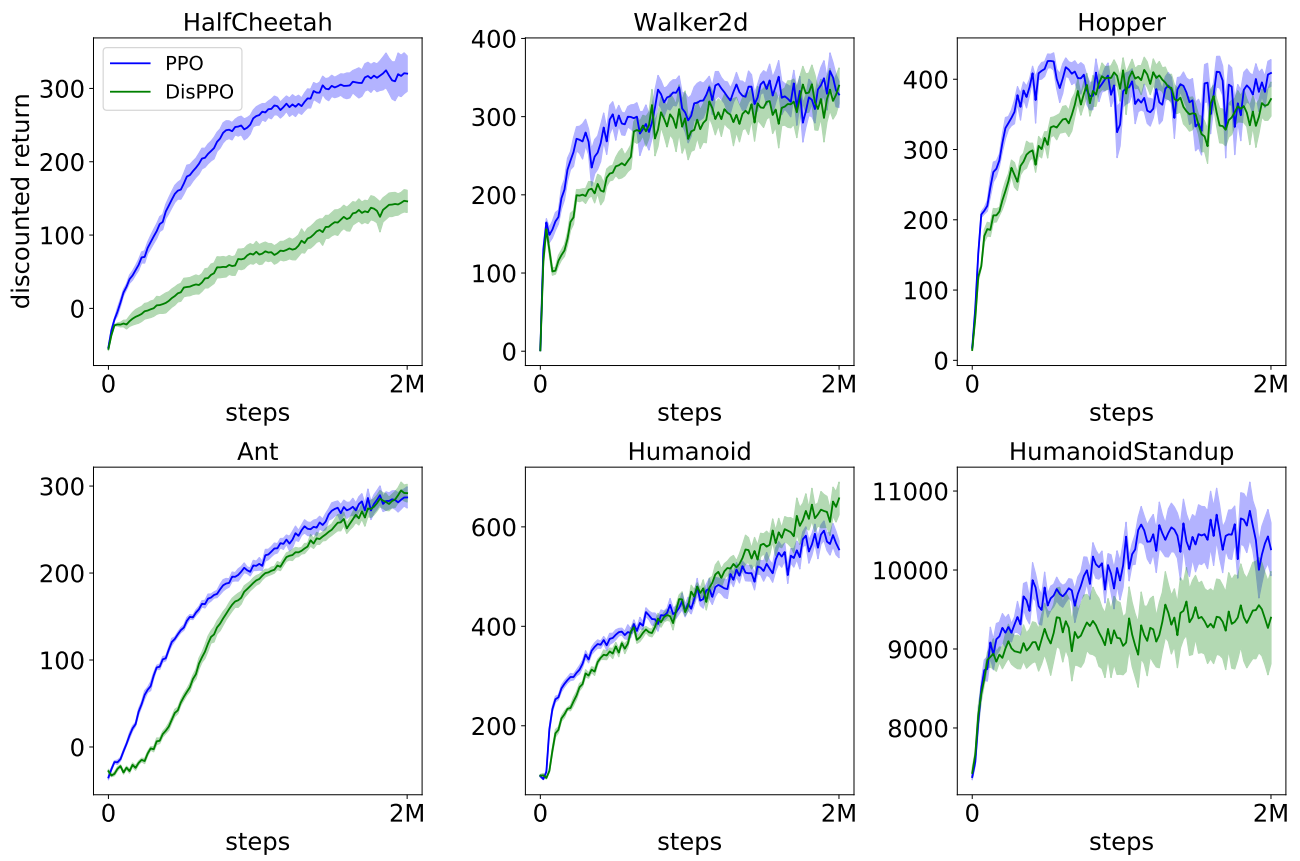


Figure 26: Comparison between PPO and DisPPO with $\gamma = 0.995$. The larger version of Figure 10.

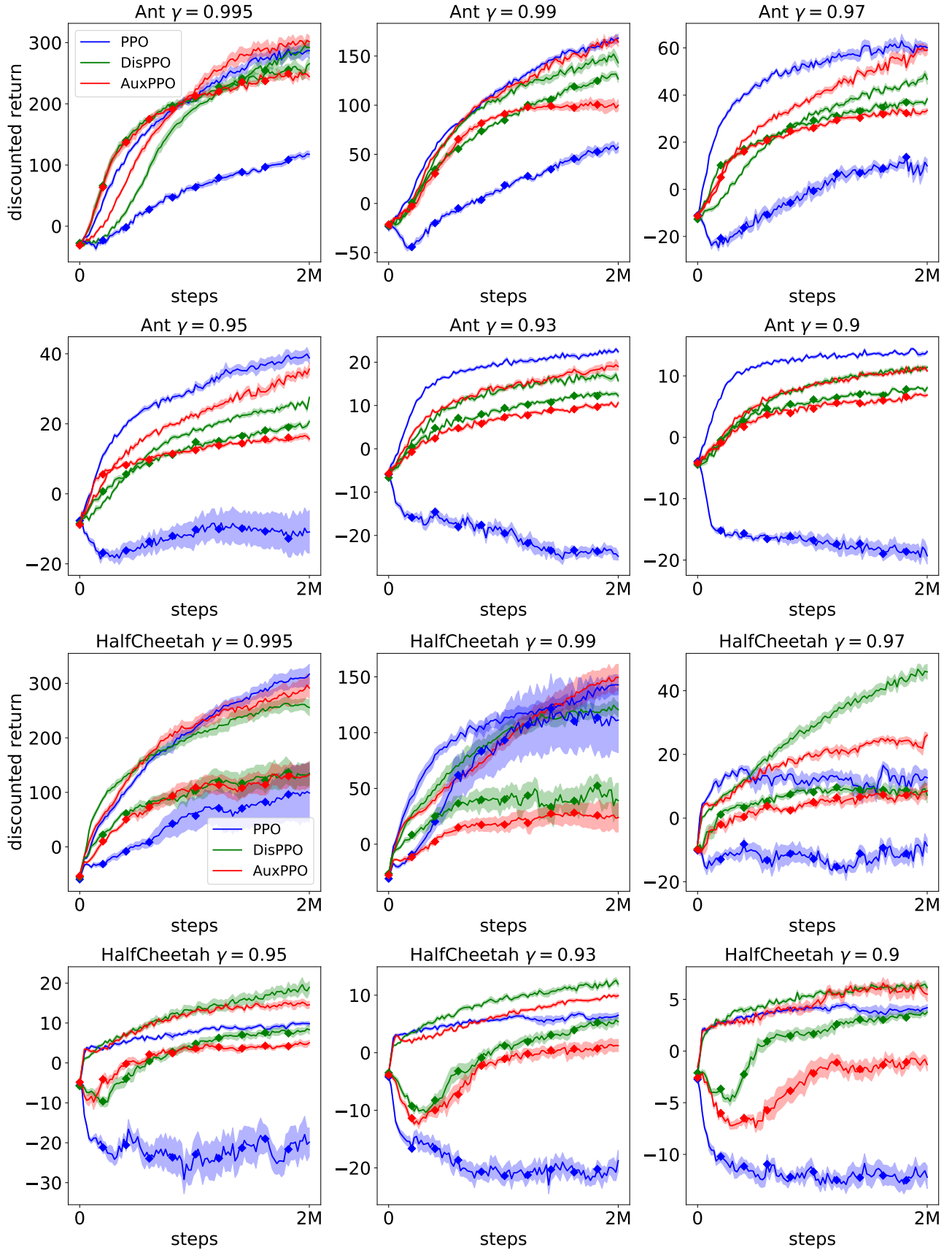


Figure 27: Curves without any marker are obtained in the original Ant environment. Diamond-marked curves are obtained in Ant with r' . The larger version of Figure 11.